

Z' Mediated WIMPs: Dead, Dying, or Soon to be Detected?

Carlos Blanco,^{1,2} Miguel Escudero,³ Dan Hooper,^{2,4,5} and Samuel J. Witte⁶

¹*University of Chicago, Department of Physics, Chicago, IL 60637, USA*

²*University of Chicago, Kavli Institute for Cosmological Physics, Chicago, IL 60637, USA*

³*King's College London, Department of Physics, Strand, London WC2R 2LS, UK*

⁴*Fermi National Accelerator Laboratory, Theoretical Astrophysics Group, Batavia, IL 60510, USA*

⁵*University of Chicago, Department of Astronomy and Astrophysics, Chicago, IL 60637, USA*

⁶*Instituto de Física Corpuscular (CSIC-Universitat de València), Paterna (Valencia), Spain*

E-mail: carlosblanco2718@uchicago.edu, miguel.escudero@kcl.ac.uk,
dhooper@fnal.gov, sam.witte@ific.uv.es

ABSTRACT: Although weakly interacting massive particles (WIMPs) have long been among the most studied and theoretically attractive classes of candidates for the dark matter of our universe, the lack of their detection in direct detection and collider experiments has begun to dampen enthusiasm for this paradigm. In this study, we set out to appraise the status of the WIMP paradigm, focusing on the case of dark matter candidates that interact with the Standard Model through a new gauge boson. After considering a wide range of Z' mediated dark matter models, we quantitatively evaluate the fraction of the parameter space that has been excluded by existing experiments, and that is projected to fall within the reach of future direct detection experiments. Despite the existence of stringent constraints, we find that a sizable fraction of this parameter space remains viable. More specifically, if the dark matter is a Majorana fermion, we find that an order one fraction of the parameter space is in many cases untested by current experiments. Future direct detection experiments with sensitivity near the irreducible neutrino floor will be able to test a significant fraction of the currently viable parameter space, providing considerable motivation for the next generation of direct detection experiments.

Contents

1	Introduction	1
2	Z' Mediated Dark Matter Models	3
2.1	Dirac Dark Matter	3
2.2	Majorana Dark Matter	3
2.3	Loop-Induced Kinetic Mixing	4
3	Dark Matter Phenomenology	4
3.1	Model Requirements	5
3.2	Constraints from Cosmology	5
3.3	Direct Detection	6
3.4	Indirect Detection	6
3.5	Collider, Fixed Target and Neutrino Experiments	7
3.6	Reach of Future Direct Detection Experiments	7
4	Results	9
4.1	Dirac Dark Matter	9
4.1.1	Couplings to Quarks	9
4.1.2	Couplings to Leptons	12
4.2	Majorana Dark Matter	19
4.2.1	Couplings to Quarks	19
4.2.2	Couplings to Leptons	21
5	Caveats and Theoretical Considerations	28
5.1	Models With an Axial Z'	28
5.2	UV Complete Models	28
6	Implications for the WIMP Paradigm	29
7	Discussion and Summary	32
A	Partial Wave Unitarity	46

1 Introduction

Over the past several decades, the most popular and well-studied candidates for dark matter have been stable particles that were in equilibrium with the Standard Model (SM) bath in the early universe and that then froze-out to yield a thermal relic abundance in agreement with the measured cosmological dark matter density. In order for this process to result in an acceptable dark matter abundance, such particles were generally required to possess very roughly weak-scale masses and couplings to the SM. This result provided the foundation for what has become known as the WIMP paradigm.

It has long been appreciated that if the dark matter consists of weakly interacting massive particles (WIMPs), it should be possible to detect these particles through their elastic scattering with nuclei, by observing their annihilation products, or by producing them in colliders (for recent reviews, see Refs. [1–3]). With this goal in mind, large and highly sensitive underground detectors have been developed and deployed, resulting in very stringent limits on the dark matter’s scattering cross section with nuclei [4–8]. The Large Hadron Collider (LHC) has also begun to explore the electroweak-scale, but has not identified any evidence that dark matter particles are being produced in these collisions [9–19]. Lastly, while the Galactic Center gamma-ray excess [20–28] and the cosmic-ray antiproton excess [29–32] are each suggestive of originating from dark matter annihilation, no consensus has emerged regarding the interpretation of this data. These results have motivated many scientists working on the problem of dark matter to consider alternatives to the WIMP paradigm [33], elevating the degree of interest being directed towards candidates such as axions [34–40], as well as scenarios in which the dark matter is part of a hidden sector [41–58].

At this point in time, it is not entirely clear how one should view the status of the WIMP paradigm. On the one hand, it is certainly the case that many once attractive dark matter candidates have been excluded by the null results of direct detection experiments and by searches for new physics at the LHC [59–61]. It is also true, however, that many varieties of WIMPs remain entirely viable [62–65]. How one thinks about the relative weighting of these scenarios impacts how we should devote our experimental and theoretical resources. With so much at stake, we would ideally attempt to make a systematic and thorough assessment of the current status of the WIMP paradigm. Given the vast diversity of possible WIMP models that one could consider, however, a truly exhaustive study would be an enormous and practically intractable undertaking. With such considerations in mind, we have chosen to focus more narrowly in this study on the case of dark matter particles that annihilate through couplings to a new vector gauge boson, Z' [66–83]. New broken $U(1)$ gauge symmetries and the Z' bosons that accompany them are found within many well-motivated extensions of the SM [84], including many Grand Unified Theories (GUTs) [85, 86] and string-inspired models [87–95], as well as within the context of dynamical symmetry breaking scenarios [96–98], models with extra spatial dimensions [99–102], and many other popular extensions of the SM [103–109]. Within this relatively simple subset of WIMP models, we will consider scenarios in which the dark matter candidate is either a Majorana or Dirac fermion, and Z' bosons that possess a wide range of couplings and other characteristics. This collection of well-motivated models can lead to a wide range of phenomenological consequences, with detection prospects that vary from easily testable, to extremely elusive.

The remainder of this study is structured as follows. In Sec. 2, we describe the range of Z' mediated dark matter models that we will consider in this study. We then describe in Sec. 3 the current and projected constraints that we apply to this class of models. In Sec. 4 we present our main results. After discussing some caveats and other theoretical considerations in Sec. 5, we attempt in Sec. 6 to quantitatively evaluate the status of Z' mediated WIMPs. To this end, we perform a Bayesian analysis, calculating for each given model (and for three choices of priors) the fraction of the parameter space that has been ruled out by existing experiments, as well as the fraction that is projected to fall within the reach of future direct detection experiments. Although the current constraints do exclude a significant fraction of the Z' mediated dark matter parameter space, a sizable proportion remains viable (in the case that the dark matter is a Majorana fermion). The prospects for future direct detection experiments are quite encouraging; we project that experiments with sensitivity near the neutrino floor will be able to test a significant fraction of the currently viable parameter space. We discuss and summarize our results in Sec. 7.

2 Z' Mediated Dark Matter Models

In this section, we describe the range of Z' mediated dark matter models considered in this study. In order to ensure maximum generality, we have taken a simplified models approach, in which we describe the masses and couplings of the dark matter and Z' without necessarily specifying the full particle content of the underlying theory. Although one might ideally like to consider models that are UV complete and fully gauge invariant [77, 110–125], this comes at the cost of significantly increasing the dimensionality of the parameter space. Here, we will consider models that respect the symmetries of the SM and maintain tree-level gauge invariance, but do not explicitly require the cancellation of gauge anomalies. Within the context of such models, we assume that loop-level gauge invariance is achieved through the presence of additional unspecified particles, which do not play a significant role in the dark matter phenomenology under consideration. For additional discussion, see Sec. 5.

2.1 Dirac Dark Matter

The simplest realization containing a Dirac dark matter candidate, χ , arises when the Z' acquires its mass through the Stueckelberg mechanism (see, for example, Ref [126]). Here, the Lagrangian is extended by the following (neglecting the dark matter kinetic term):

$$\mathcal{L} \supset - \sum_i g' q_i Z'_\mu \bar{f}_i \gamma^\mu f_i + m_\chi \bar{\chi} \chi - \frac{\epsilon}{4} F^{\mu\nu} F'_{\mu\nu} - \frac{1}{4} F'^{\mu\nu} F'_{\mu\nu}, \quad (2.1)$$

where the sum is performed over all SM fermions as well as the dark matter candidate. The quantities g' , $F'_{\mu\nu}$ and q_i are the gauge coupling, field strength tensor, and charge assignments of the $U(1)'$, respectively. The kinetic mixing between the $U(1)'$ and $U(1)_Y$ is quantified by ϵ , which we take to be zero at tree-level (but is induced through loops, as described in Sec. 2.3). For simplicity, we will often refer to the interactions of the Z' in terms of its effective universal coupling to SM fermions, $g_{SM} \equiv q_i g'$ (where i includes all SM fermions that are charged under the $U(1)'$), and its coupling to the dark matter, $g_\chi \equiv q_\chi g'$.

2.2 Majorana Dark Matter

In the case of dark matter in the form of a Majorana fermion, one cannot simply exploit the Stueckelberg mechanism, as simplified Z' models with non-zero axial couplings naturally violate unitarity at high energies [127]. This problem can be circumvented, however, if one instead generates the necessary masses through the spontaneous breaking of the $U(1)'$ symmetry by a new SM singlet scalar, ϕ , which we take here to be complex and charged under the new $U(1)'$ with $q_\phi = 2q_\chi$. Specifically, we will assume that the Lagrangian in the unbroken phase contains the following terms:

$$\begin{aligned} \mathcal{L} \supset & - \sum_i g' q_i Z'_\mu \bar{f}_i \gamma^\mu f_i - \frac{1}{2} g' q_\chi Z'_\mu \bar{\chi} \gamma^\mu \gamma_5 \chi - \frac{\lambda_\chi}{\sqrt{2}} (\phi \bar{\chi} \chi^c + h.c.) \\ & + (D_\mu \phi)^\dagger D^\mu \phi + \mu_\phi^2 \phi^\dagger \phi - \lambda_\phi (\phi^\dagger \phi)^2 - \lambda_{H\phi} H^\dagger H \phi^\dagger \phi - \frac{\epsilon}{4} F^{\mu\nu} F'_{\mu\nu} - \frac{1}{4} F'^{\mu\nu} F'_{\mu\nu}, \end{aligned} \quad (2.2)$$

where λ_χ is a Yukawa coupling, μ_ϕ^2 and λ_ϕ are parameters in the scalar potential, and $\lambda_{H\phi}$ is the scalar-Higgs mixing. We again take ϵ to be zero at tree-level, and additionally assume that the scalar-Higgs mixing vanishes ($\lambda_{H\phi} = 0$). Spontaneous symmetry breaking causes the scalar to develop a vacuum expectation value, v' . In the unitary gauge, one can rewrite the field as $\phi = \frac{1}{\sqrt{2}}(v' + \rho)$, where ρ is a CP-even scalar field. Minimization of the scalar potential yields $\mu_\phi^2 = \lambda_\phi v'^2$. By substituting

$\phi = \frac{1}{\sqrt{2}}(v' + \rho)$ into Eq. 2.2, together with $D_\mu\phi = \partial_\mu\phi - ig'2q_\chi Z'_\mu\phi$, one finds that the resulting Lagrangian contains:

$$\begin{aligned} \mathcal{L} \supset & - \sum_i g' q_i Z'_\mu \bar{f}_i \gamma^\mu f_i - g' \frac{q_\chi}{2} Z'_\mu \bar{\chi} \gamma^\mu \gamma_5 \chi - \frac{\lambda_\chi}{2} (v' + \rho) \bar{\chi} \chi \\ & + \frac{1}{2} \partial_\mu \rho \partial^\mu \rho + 2g'^2 q_\chi^2 Z'_\mu Z'^\mu (v'^2 + 2v'\rho + \rho^2) - \frac{1}{4} \lambda_\phi (\rho + v')^2 (\rho^2 + 2\rho v' - v'^2). \end{aligned} \quad (2.3)$$

In the broken phase, the mass of the dark matter, new gauge boson, and real scalar can be expressed as follows: $m_\chi = \lambda_\chi v'$, $m_{Z'} = 2q_\chi g' v'$ and $m_\rho^2 = 2\lambda_\phi v'^2$. Substituting in these mass parameters, one arrives at:

$$\begin{aligned} \mathcal{L} \supset & - \sum_i g' q_i Z'_\mu \bar{f}_i \gamma^\mu f_i - g' \frac{q_\chi}{2} Z'_\mu \bar{\chi} \gamma^\mu \gamma_5 \chi - \frac{m_\chi}{2} \left(1 + \frac{\rho}{v'}\right) \bar{\chi} \chi \\ & + \frac{1}{2} \partial_\mu \rho \partial^\mu \rho + \frac{m_{Z'}^2}{2} Z'_\mu Z'^\mu \left(1 + \frac{\rho}{v'}\right)^2 - \frac{m_\rho^2}{8v'^2} \rho^2 (\rho + 2v')^2. \end{aligned} \quad (2.4)$$

In order to minimize its impact of the resulting phenomenology, we will take the mass of the scalar to be equal to the maximum value consistent with unitarity, $m_\rho = \sqrt{\pi} m_{Z'}/g_\chi$ (see Appendix A).

2.3 Loop-Induced Kinetic Mixing

Kinetic mixing between the $U(1)'$ and $U(1)_Y$ can shift the mass and couplings of the Z from their predicted value [128], and thus precision electroweak measurements can be used to constrain the value of ϵ [129–131]. With this in mind, we assume throughout this study that ϵ vanishes at tree level, but is generated at loop level, yielding the following [132, 133]:

$$\epsilon \sim \frac{g_Y g'}{12\pi^2} \sum_i Y_i q_i \ln \left(\frac{\Lambda^2}{m_{f_i}^2} \right), \quad (2.5)$$

where g_Y is the SM gauge coupling, Y_i is the hypercharge of fermion i , and $\Lambda = m'_{Z'}/\sqrt{g_\chi g_f}$ is the effective cutoff scale.

In addition to any tree-level couplings that may exist, kinetic mixing will induce an effective coupling of the Z' to SM fermions: $\mathcal{L} \in -g_Y \cos\theta_W \epsilon \bar{f} \gamma_\mu f Z'_\mu$, where $\epsilon \simeq g_{SM} g_Y \cos\theta_W / 4\pi^2 \sim 10^{-2} g_{SM}$. These loop-induced couplings will play an important role in determining many of the constraints presented in this study and are included in all of the relevant calculations presented here.

3 Dark Matter Phenomenology

In this section, we describe our analysis of the Z' mediated dark matter models presented in the previous section. In order to make this problem more tractable, we will limit our analysis to the following sets of $U(1)'$ charge assignments:

- Coupling to lepton number, with $q_l = 1$ for all SM leptons.
- Coupling only to first-generation leptons, with $q_e = q_{\nu_e} = 1$.
- Coupling only to third-generation leptons, with $q_\tau = q_{\nu_\tau} = 1$.
- Coupling to baryon number, with $q_q = 1/3$ for all SM quarks.

- Coupling only to first-generation quarks, with $q_u = q_d = 1/3$.
- Coupling only to third-generation quarks, with $q_t = q_b = 1/3$.

We have chosen this selection of charge assignments in order to cover a diverse and representative range of phenomenological possibilities. For example, models without tree-level couplings to SM quarks (*i.e.* “leptophilic” models) are generally less constrained by direct detection. Furthermore, models with couplings only to first or third generation fermions can lead to very different annihilation cross sections and scattering rates with nuclei (for theoretical motivation for models with couplings only to third generation fermions, see Refs. [72, 98, 134–136]). While one could easily construct a $U(1)'$ model with charge assignment that do not fall within any of the above listed examples, the phenomenology of such a model would in most cases map closely onto one or more of the models considered here.

For each choice of charge assignments, we explore a 4-dimensional parameter space in terms of m_χ , $m_{Z'}$, g_{SM} and g_χ . In each case, we consider four discrete values for g_χ/g_{SM} , equal to 10^{-2} , 10^{-1} , 1 and 10. Although these scenarios should perhaps not all be considered to be equally well-motivated, the choices of these ratios provides a broad perspective and allows one to observe how the various constraints are impacted by the choice of g_χ/g_{SM} . In general, scenarios featuring small values of g_χ/g_{SM} are more strongly constrained, while larger values make the dark matter and Z' increasingly secluded from the SM, in the limiting case constituting a hidden sector model [41–46, 48–56, 58]. For each choice of m_χ , $m_{Z'}$, g_χ/g_{SM} and charge assignments, we select the value of $g_{\text{SM}} g_\chi$ such that the thermal relic abundance is equal to the measured cosmological dark matter density, $\Omega_\chi h^2 = 0.12$ [137], as calculated using the publicly available program `micrOMEGAs` (version 5.0.4) [138]. We then assess whether a given point in parameter space is consistent with the constraints from direct detection, indirect detection, measurements of the cosmic microwave background (CMB), and a variety of collider, fixed target and neutrino experiments.

3.1 Model Requirements

Throughout this study, we will remain largely agnostic regarding the masses and couplings of the dark matter candidate and the Z' . There are, however, a number of model independent requirements that we can impose on these parameters. Firstly, we require that partial wave unitarity is respected, as described in Appendix A. We also require each coupling in the theory to be smaller than $\sqrt{4\pi}$, in order to maintain perturbativity. And lastly, we require that the width of the Z' does not exceed 10% of its mass, $\Gamma_{Z'} < 0.1 m_{Z'}$.¹

3.2 Constraints from Cosmology

Measurements of the temperature anisotropies in the cosmic microwave background (CMB) and of the primordial light nuclei abundances enable us to place important constraints on the parameter space within this class of models. In particular, throughout this study we will consider only parameter space with $m_\chi, m_{Z'} \gtrsim 10$ MeV, in order to avoid conflict with the successful predictions of Big Bang Nucleosynthesis (BBN) [139–141].

The annihilation of dark matter particles in the era leading up to and after recombination can have an observable impact on the CMB. More specifically, the annihilation products can produce large

¹Dark matter annihilation cross sections are computed in `micrOMEGAs` [138] under the assumption that all particles involved in the annihilation processes have a narrow width. Therefore, for consistency, we require the width of the Z' not to exceed 10% of its mass, $\Gamma_{Z'} < 0.1 m_{Z'}$. Furthermore, since $\Gamma_{Z'} \sim g^2/(8\pi) m_{Z'}$, regions of parameter space in which $\Gamma_{Z'} > 0.1 m_{Z'}$ correspond to $g \gtrsim 0.45 \times \sqrt{4\pi}$, only marginally consistent with the requirement of perturbativity.

numbers of ionizing photons, which increase the fraction of free electrons in the universe. This has a direct impact on the integrated optical depth as observed by Planck, which directly constrains the annihilation power at the 95% CL, defined as [137]:

$$p_{\text{ann}} \equiv f_{\text{eff}} \frac{\langle \sigma v \rangle}{m_\chi} < 3.4 \times 10^{-28} \text{ cm}^3/\text{s}/\text{GeV}, \quad (3.1)$$

where the effective efficiency factor, f_{eff} , is the fraction of the annihilation power that is transferred into the intergalactic medium during the relevant range of redshifts [137, 142]. For a given model, we calculate f_{eff} by integrating the e^\pm and gamma-ray annihilation spectra as calculated by `micrOMEGAs` [138] (utilizing `PYTHIA` [143]) over the precalculated $f_{\text{eff}}^{e^\pm, \gamma}$ curves provided in Ref [144]:

$$f_{\text{eff}}(m_\chi) = \frac{1}{2m_\chi} \int_0^{m_\chi} \left(f_{\text{eff}}^e \frac{dN_e}{dE_e} + f_{\text{eff}}^\gamma \frac{dN_\gamma}{dE_\gamma} \right) E dE. \quad (3.2)$$

This procedure yields a bound that generally rules out s -wave annihilating dark matter with $m_\chi \lesssim 10 - 20$ GeV (see, however, Ref. [145]).

3.3 Direct Detection

Searches for the elastic (or inelastic) scattering of dark matter particles with nuclei have provided some of the most powerful constraints on WIMPs. In recent years, experiments utilizing a target of liquid xenon (including XENON1T [4, 7], LUX [5, 8], and PandaX-II [6]) have placed the most stringent constraints on such interactions across much of the relevant parameter space.

For each model under consideration, we compute the leading order scattering cross section and compare it with the 90% CL upper limit obtained from the aforementioned experiments. In cases in which this interaction occurs at tree level, the cross section is computed using `micrOMEGAs`. In models in which the Z' does not couple to quarks, however, scattering with nuclei only occurs through loop-induced interactions arising from kinetic mixing. Such scattering is dominated by the heaviest charged lepton that couples to the Z' , and leads to the following cross section for the cases of Dirac and Majorana dark matter, respectively [133]:

$$\begin{aligned} \sigma_{\text{Dirac}} &= \frac{\mu_N^2}{9\pi} \left[\frac{\alpha_{\text{EM}} Z}{\pi \Lambda^2} \log \left(\frac{m_\ell^2}{\Lambda^2} \right) \right]^2, \\ \sigma_{\text{Majorana}} &= \frac{\mu_N^2 v_\chi^2}{9\pi} \left(1 + \frac{\mu_N^2}{2m_N^2} \right) \left[\frac{\alpha_{\text{EM}} Z}{\pi \Lambda^2} \log \left(\frac{m_\ell^2}{\Lambda^2} \right) \right]^2, \end{aligned} \quad (3.3)$$

where $\mu_N \equiv m_N m_\chi / (m_N + m_\chi)$ is the reduced mass of the nucleus-dark matter system, Z is the charge of the nucleus, $v_\chi \sim 10^{-3} c$ is the velocity of the dark matter, and $\Lambda = m_{Z'}/\sqrt{g_\chi g_l}$.

3.4 Indirect Detection

Indirect searches include efforts to detect the gamma rays, antiprotons, positrons, neutrinos and other particles that are produced in the annihilations (or decays) of dark matter particles. In this study, we apply constraints as derived from gamma-ray observations of the Milky Way's dwarf spheroidal galaxies by the Fermi telescope [146] and measurements of the cosmic-ray e^\pm spectrum by AMS-02 [147, 148].

To apply these constraints, we use `micrOMEGAs` to calculate the spectrum of gamma rays, electrons and positrons that are produced per annihilation in a given model and compare with the 95% CL upper limits obtained from Fermi-LAT and AMS-02. There is a high degree of complementarity between

these measurements, as Fermi is most sensitive to annihilations that produce quarks or tau leptons, while AMS-02 yields its strongest constraints in the case of annihilations to muons or electrons. In models in which $m_\chi > m_{Z'}$ and $g_\chi \gg g_{\text{SM}}$, the t -channel annihilation into a pair of on-shell Z' bosons can be the dominant annihilation channel. In this case, the boosted decay of the Z' annihilation products leads to a rather smooth e^\pm spectrum, without the distinctive spectral features that are present in models featuring direct annihilation to e^+e^- or $\mu^+\mu^-$ [149, 150]. In this case, the AMS-02 constraints are significantly weakened, and are not included here.

3.5 Collider, Fixed Target and Neutrino Experiments

The results of accelerator experiments have been used to place stringent constraints on the mass and couplings of a Z' . For relatively heavy Z' bosons, some of the strongest limits come from searches for dijet resonances at experiments including CMS, ATLAS, CDF and UA2 [151–157]. Such searches provide particularly stringent constraints on the couplings of a Z' to quarks. Searches at the LHC for dilepton resonances also broadly constrain models in which the Z' couples more strongly to charged leptons [158, 159]. We apply these constraints rescaling the bounds derived in Ref. [122] by the appropriate model-dependent production factor and branching ratios. We also apply constraints derived from the measurement of LEP, which strongly limit the couplings of a Z' to electrons. For $m_{Z'} \gtrsim 200$ GeV, LEP provides a limit of $g_e < (m_{Z'}/7 \text{ TeV})$ [160].

For the case of a lighter Z' , a wide range of constraints have been derived from the results of collider and beam dump experiments, including BaBar, NA48/2, LHCb, KLOE, NA64, as well as electron and proton beam dumps [161–188]. We apply this collection of constraints to the specific Z' models considered here using the DarkCast software [189]. In addition, we also apply the following constraints on the couplings to leptons as derived from Borexino data [190]: $g_e < 5 \times 10^{-3} (m_{Z'}/\text{GeV})$ [191] and $(g_{\mu,\tau} \epsilon g_Y \cos \theta_W)^{1/2} < 5 \times 10^{-3} (m_{Z'}/\text{GeV})$ [192]. These constraints account for the effects of kinetic mixing as well as the fact that roughly 33% of the solar neutrino flux is of each flavor.

Note that the constraints obtained from the LHC, DarkCast, and Borexino do not appear in the summary plots of the Dirac dark matter candidates; this is not to suggest that they don't apply or exist, but rather this is a reflection of the fact that the parameter space probed by these sources is excluded by a combination of other experiments.

All of the limits from collider, fixed target, and neutrino experiments are quoted at the 95% CL.

3.6 Reach of Future Direct Detection Experiments

Direct detection experiments will ultimately encounter an irreducible background arising from the coherent scattering of the ambient neutrino background [193, 194]. This background of neutrinos is produced from various sources, including nuclear reactions in the Sun [195, 196], interactions of cosmic rays in the atmosphere [197], galactic supernovae [198, 199]², nuclear fission reactors [206–208], and decays of radioactive elements in the Earth [209, 210]. The signature produced by the coherent scattering of these neutrinos is remarkably similar to what is naively expected for dark matter, and will consequently inhibit the ability of direct detection experiments to probe new parameter space. It is important to emphasize, however, that the so-called “neutrino floor” is not entirely impregnable, as the spectrum of recoils produced by coherent neutrino scattering is, in general, not entirely degenerate with the recoil spectrum predicted from dark matter. Experiments can thus, in principle, attempt to

²Typically only the diffuse isotropic supernovae background is included in calculations of neutrino background. Should a local star core collapse, however, pre- [200] and post-supernovae [201–205] neutrinos may also contribute. Since these signals are rare and strongly time-dependent, we neglect these contributions in what follows.

Target	Exposure [tonne-year]	E_{th} [keV]	E_{max} [keV]
Argon G3 (ARGO)	10^3	10.0	150
Argon G3 (ARGO S2)	10^3	0.6	10
Xenon G3 (DARWIN)	200	1.0	150
Fluorine G3 (PICO-500)	2	6.0	150
Germanium G3 (SuperCDMS+)	5	0.04	50

Table 1. Configurations adopted for our projection of neutrino-floor direct detection experiments. The projected sensitivities of these experiments are shown in Fig. 1.

subtract this background [193, 194, 211, 212]. In this regime, however, constraints on the cross section would be expected to scale more slowly with exposure. It is thus unclear as to whether there will exist sufficient motivation to build experiments that are capable of significantly cutting into the neutrino floor. For the purposes of this work, we will define the final stage of direct detection as the maximally optimistic realizations of currently proposed experiments. We describe these experiments below, and summarize their properties in Table 1.

Argon G3: The most futuristic proposal made by the DarkSide collaboration is the construction of a 300 tonne (200 tonne fiducial volume) argon time projection chamber that would operate for up to five years (this proposal is being referred to “ARGO”) [213, 214]. We adopt two different operating thresholds for this experiment, one consistent with the high-energy regime outlined in the ARGO proposal, the other being a low-mass search consistent with the recent analysis performed by the Darkside-50 collaboration [215].

Xenon G3: The XENON collaboration has proposed an experiment, referred to as “DARWIN”, intended to extend in sensitivity all the way to the atmospheric neutrino background. The current proposal assumes a 40 tonne fiducial volume of liquid xenon operating for five years [216]. The current design documents list a threshold of ~ 5 keV, adopted in order to avoid the solar neutrino background at low energies (current xenon experiments achieve an absolute threshold closer 1.1 keV, albeit with limited efficiency) [4–6, 217]. We optimistically adopt a threshold of 1 keV, although we emphasize that the constraints we derive at low masses from other experiments are more stringent, and thus our results are not strongly sensitive to this choice.

Fluorine G3: The conceptual design for the construction of PICO-500, a ~ 500 kg fiducial volume bubble chamber, has recently been approved by SNOLAB [218, 219]. In our calculations we adopt a 6 keV threshold and a 2 tonne-year exposure, although we emphasize that our final result is only slightly sensitive to these choices, as the spin-dependent bound derived from the Xenon G3 experiment is typically stronger for models in which the Z' couples equally to neutrons and protons.

Germanium G3: The CDMS collaboration has published estimated sensitivity curves for their next generation experiment, SuperCDMS SNOLAB. This experiment is expected to begin operation in 2020, and is not expected to reach the neutrino floor. Thus, we consider an advanced version of this experiment comprised of the germanium high-voltage detectors, for which the current threshold is ~ 40 eV [220], and an exposure of 5 tonne-years.

In order to project the sensitivity of the above described experiments, we simulate neutrino events for each of the experimental realizations using the neutrino fluxes provided in [212]³, and derive

³It is worth mentioning that the flux of reactor [212], geological [221, 222], and atmospheric neutrinos [223] depend, in principle, on the geographic location of the experiment. Reactor and geological neutrinos are expected to be a

90% upper limits on the direct detection cross sections using an extended likelihood function. This procedure is repeated 10^3 times, each time producing new realizations of the neutrino data. For each dark matter mass and interaction, we identify the minimum cross section constrained by at least 90% of the realizations. These projected bounds represent our effective neutrino floor, and are shown in Fig. 1 for the case of equal couplings to protons and neutrons.

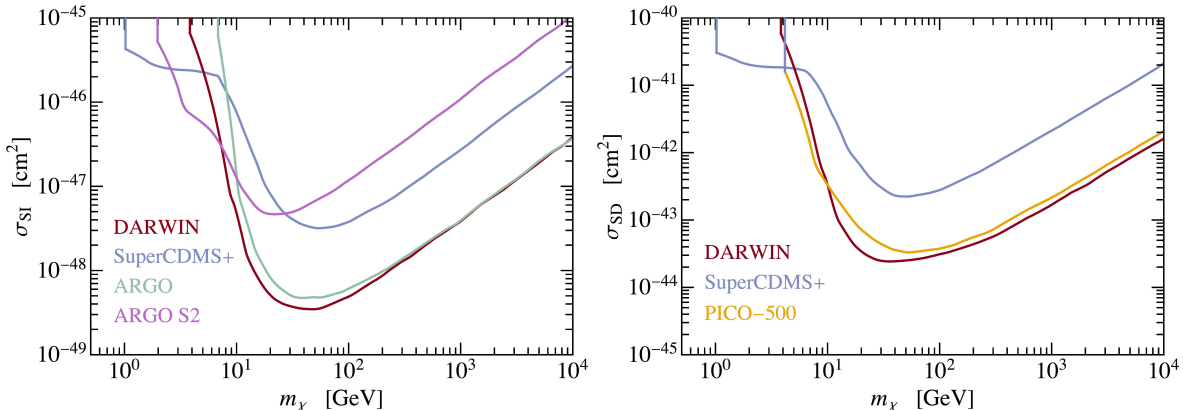


Figure 1. The projected neutrino-floor sensitivity for several direct detection experiments, for the case of equal couplings to protons and neutrons. Constraints are shown for spin-independent (left) and spin-dependent (right) scattering.

4 Results

4.1 Dirac Dark Matter

In this section, we consider the case of dark matter in the form of a Dirac fermion, as described in Sec. 2.1. For each of the charge assignments described in Sec. 3, we scan over m_χ and $m_{Z'}$ and consider four discrete choices of g_χ/g_{SM} . At each point in this parameter space, we set the product of these couplings, $g_\chi g_{\text{SM}}$ such that the desired thermal relic abundance is obtained, $\Omega_\chi h^2 \simeq 0.12$.

4.1.1 Couplings to Quarks

We begin with the case of a Z' that couples equally to all SM quarks. Such a scenario could arise, for example, in a model in which baryon number is gauged [110–112, 225–227]. In such models, the dark matter annihilates to quark-antiquark pairs without velocity-suppression, leading to indirect detection constraints that are sensitive to masses up to $m_\chi \sim 60 - 70$ GeV. Even more significantly, this model features unsuppressed spin-independent scattering with nuclei, resulting in extremely stringent direct detection constraints.

subdominant background, thus we adopt the fluxes appropriate for the SNOLAB mine with the understanding that this choice will have a minimal impact on our results. For atmospheric neutrinos, we adopt the so-called FLUKA flux [224] tabulated at Kamioka Mine as this is the only location for which low energy atmospheric fluxes have been computed. It is worth noting, however, that the differences between various cites can differ by a factor of $\sim 2-3$ at low energies where the atmospheric neutrino flux is relevant for direct detection experiments [223].

Dirac Dark Matter, Couplings to all Quarks

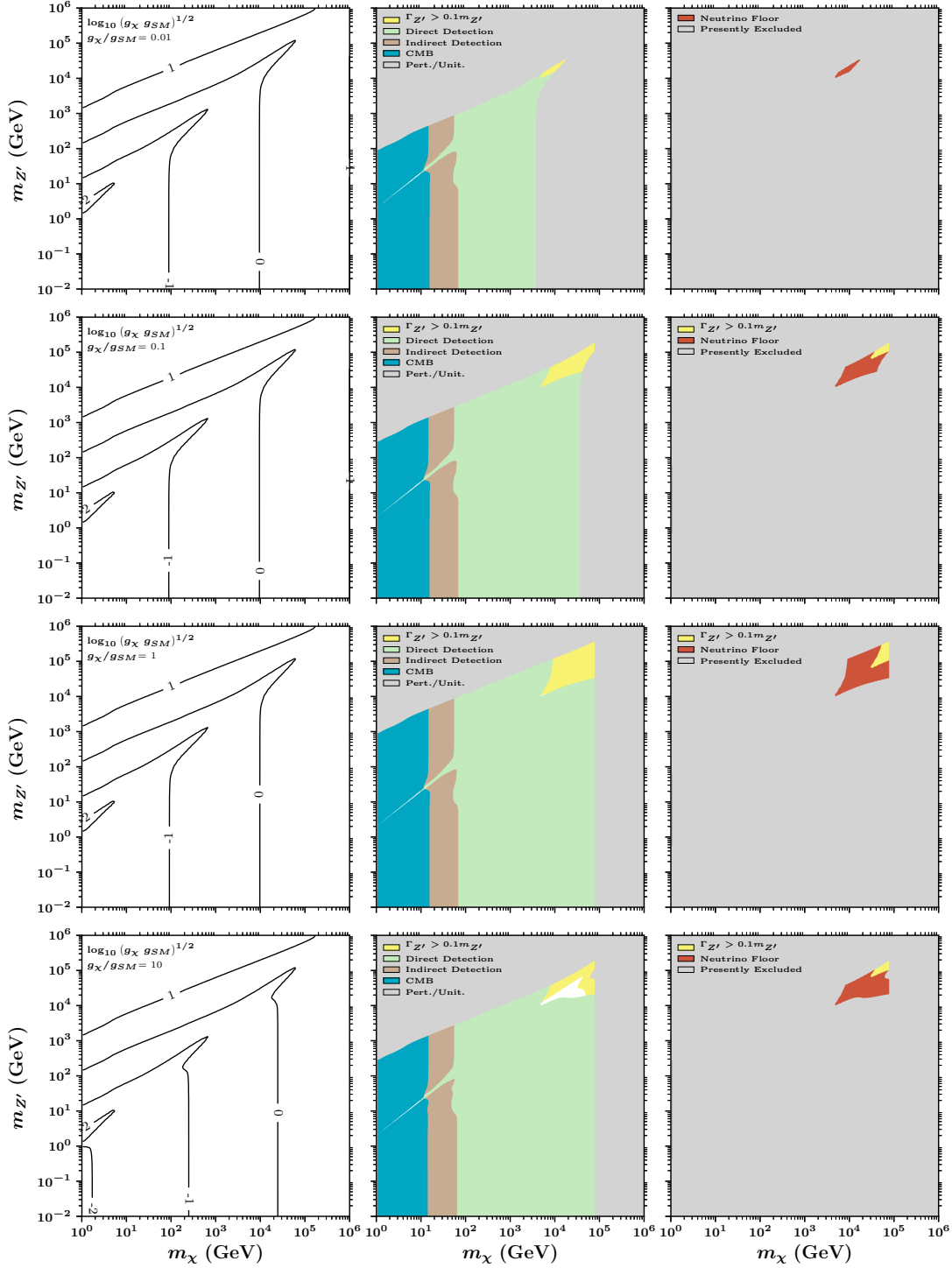


Figure 2. Constraints and prospects for detecting Dirac dark matter that is coupled to a Z' with couplings to all SM quarks. In the left frames, we plot the values of $g_\chi g_{SM}$ that yield $\Omega_\chi h^2 \simeq 0.12$. In the center and right frames, we show the current and projected constraints on this class of models, respectively. In each row, a different value of g_χ/g_{SM} has been adopted. The combined constraints from the cosmic microwave background, direct detection and indirect detection rule out the overwhelming majority of the parameter space shown. Direct detection limits are shown at the 90% CL, while all other experiments are shown at the 95% CL.

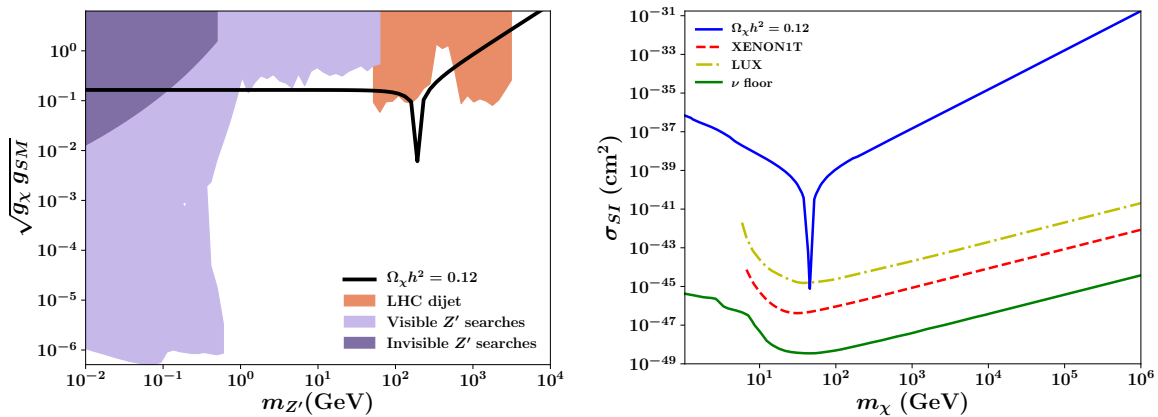


Figure 3. Left Frame: Constraints on Dirac dark matter that is coupled to a Z' with couplings to all SM quarks, for the case of $m_\chi = 100$ GeV and $g_\chi/g_{\text{SM}} = 1$. Searches for light Z' bosons [189] exclude Z' masses below ~ 1 GeV, while dijet searches at ATLAS and CMS exclude some regions of parameter space with larger values of $m_{Z'}$. Right frame: The spin-independent elastic scattering cross section with nuclei in the same model, for the case of $m_{Z'} = 100$ GeV and $g_\chi/g_{\text{SM}} = 1$. Current direct detection experiments exclude the range of models shown for all values of m_χ above the threshold for XENON1T, LUX and PandaX-II. Direct detection limits are shown at the 90% CL, while all other experiments are shown at the 95% CL.

In Fig. 2 we summarize the current and projected constraints on this class of models. In each of the left frames, we plot contours of constant $\log_{10} \sqrt{g_\chi g_{\text{SM}}}$ that yield the desired thermal relic abundance, $\Omega_\chi h^2 \simeq 0.12$. For these choices for the product of the couplings, we then plot in the center frames the current constraints on this model, as described in Sec. 3. We discard those regions labeled “Pert./Unit.” on the grounds that they are not consistent with the requirements of perturbativity and unitarity, as well as those labeled $\Gamma_{Z'} > 0.1 m_{Z'}$. The combined constraints from the cosmic microwave background, direct detection and indirect detection rule out the overwhelming majority of the parameter space of this model. The only scenarios that are not currently excluded are those in which the dark matter mass lies very near the Z' resonance ($m_{Z'} \simeq 2m_\chi$) with large values of m_χ and g_χ/g_{SM} . Although we have chosen to plot the results of this model only above $m_\chi > 1$ GeV, the constraints provided by measurements of the CMB exclude all dark matter masses below this value. Also, although collider and fixed target experiments constrain parts of the parameter space shown, those regions are also excluded by current direct detection experiments, and thus do not appear in this figure.

In the right frames of Fig. 2, we illustrate the regions of the remaining parameter space that are projected to fall within the reach of future neutrino-floor direct detection experiments, as described in Sec. 3.6. Such experiments are expected to fully explore the remaining parameter space in this case.

The constraints on this class of models are further illustrated in Fig. 3, where we plot the results across specific slices of parameter space. For the case of $m_\chi = 100$ GeV and $g_\chi/g_{\text{SM}} = 1$, searches for light Z' bosons (as characterized using DarkCast [189]) exclude Z' masses below ~ 1 GeV, while dijet searches at ATLAS and CMS exclude regions of parameter space with larger values of $m_{Z'}$. The most stringent constraints, however, are provided by direct detection experiments, which strongly exclude the range of models shown for all values of m_χ above the threshold for XENON1T, LUX and PandaX-II.

Thus far, we have considered the case in which the Z' couples equally to all SM quarks. It is,

of course, plausible that different SM quarks could possess different charges under $U(1)'$, leading to non-universal effective couplings to the Z' . In Figs. 4 and 5, we show results for the case of Dirac dark matter that is coupled to a Z' with couplings to only first or third generation quarks, respectively. In the former case, the constraints are only slightly changed, as the elastic scattering with nuclei is facilitated largely through couplings to light quarks. If the Z' only couples to third generation quarks, however, the phenomenology changes in non-negligible ways. In particular, scattering with nuclei occurs through diagrams featuring heavy quark loops, leading to somewhat smaller cross sections [228–230]. Furthermore, if $m_\chi < m_b, m_{Z'}$, the dark matter will be unable to annihilate through tree-level processes, but instead does so through loops, producing pairs of light quarks (or mesons) and leptons. If $m_\chi < m_\pi$, annihilations proceed to light leptons through an s -wave amplitude, a scenario that is excluded by measurements of the CMB. Between the mass of the pion and ~ 2 GeV, a large variety of meson annihilation channels are possible, many of which are similarly excluded. Finally, between ~ 2 GeV and the b -quark mass, annihilations will generate light quarks and leptons, and are again strongly constrained. Although we do not explicitly calculate the many hadronic annihilation processes that are relevant in this region of parameter space, we are confident that it is strongly excluded by CMB measurements and indirect detection. We denote this excluded region in red in Fig. 5.

4.1.2 Couplings to Leptons

Next, we turn our attention to the case of Dirac dark matter that is coupled to a Z' with couplings to SM leptons. We show our results for this case in Figs. 6 and 7, where once again we find that the combined constraints from the cosmic microwave background, direct detection and indirect detection rule out the overwhelming majority of the parameter space, and that the remaining parameter space is projected to fall within the reach of future direct detection experiments. Constraints from Borexino [191] also exclude much of the parameter space in this scenario.

It is worth noting that direct detection constraints in high mass parameter space appear to only be minimally suppressed, if at all, with respect to the scenario in which the Z' couplings directly to quarks, despite the interaction being loop suppressed. We note that this is consequence of the fact that the logarithm in Eq. (2.5) in this parameter space is quite large, given that $\Lambda = m_{Z'}/\sqrt{g_\chi g_f} \gg m_\ell$. At lower masses – where the logarithm is $\mathcal{O}(1)$, the direct detection bounds overlap strongly with those from indirect detection and the CMB, and thus making a straightforward comparison more difficult.

In Figs. 8 and 9, we show results for the case of Dirac dark matter that is coupled to a Z' with couplings to only first or third generation leptons, respectively. In each case, we find that the vast majority of the parameter space is currently excluded, and that future direct detection experiments are projected to cover the remaining models.

Dirac Dark Matter, Couplings to First Generation Quarks

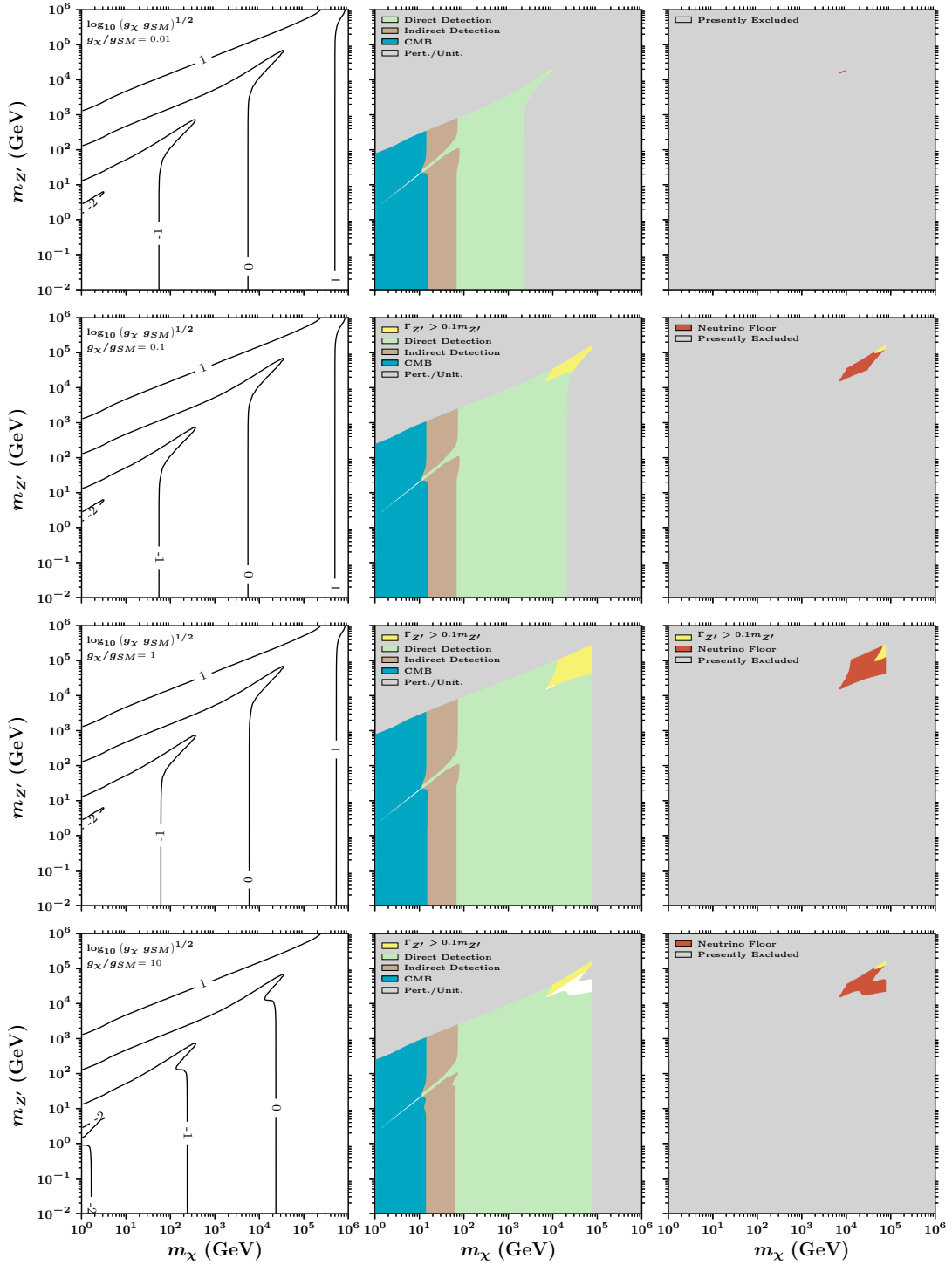


Figure 4. As in Fig. 2, but for the case of Dirac dark matter that is coupled to a Z' with couplings only to first generation quarks.

Dirac Dark Matter, Couplings to Third Generation Quarks

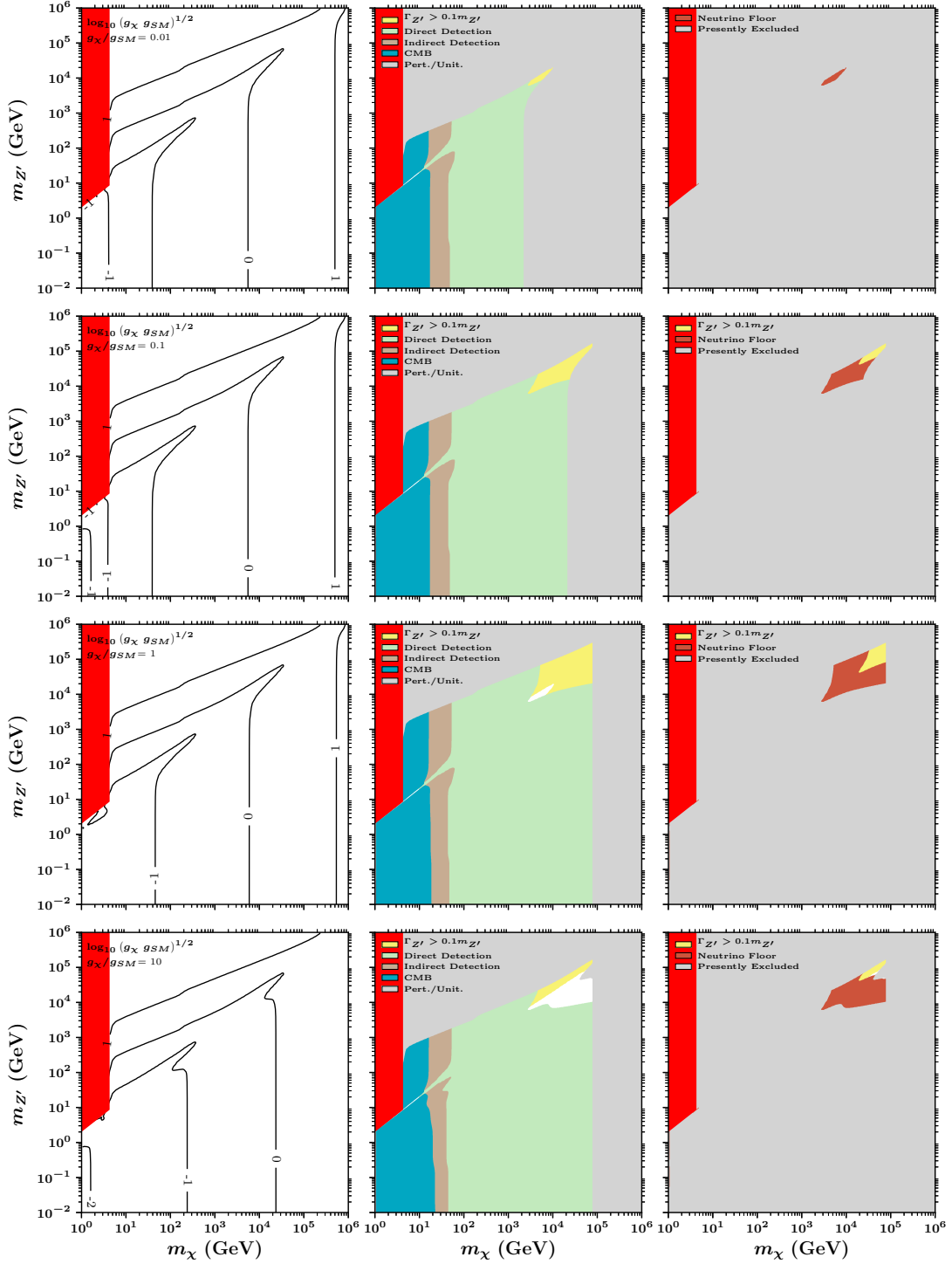


Figure 5. As in previous figures, but for the case of Dirac dark matter that is coupled to a Z' with couplings only to third generation quarks. In the red regions, annihilations produce a variety of hadronic final states without velocity suppression, and are thus ruled out by a combination of CMB measurements and indirect searches.

Dirac Dark Matter, Couplings to all Leptons

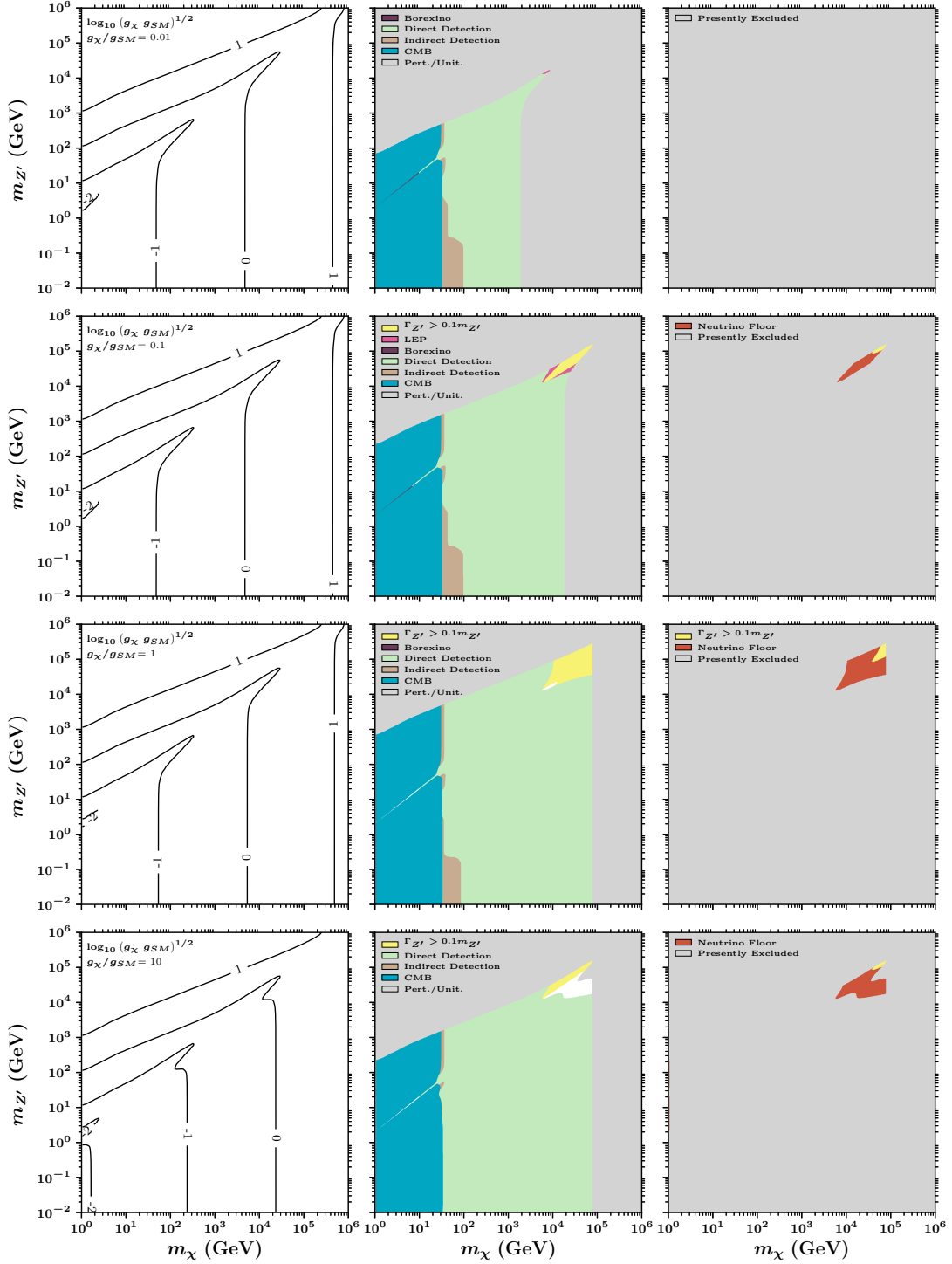


Figure 6. As in previous figures, but for the case of Dirac dark matter that is coupled to a Z' with couplings to SM leptons. Again we find that the combined constraints from the cosmic microwave background, direct detection and indirect detection rule out the overwhelming majority of the parameter space shown.

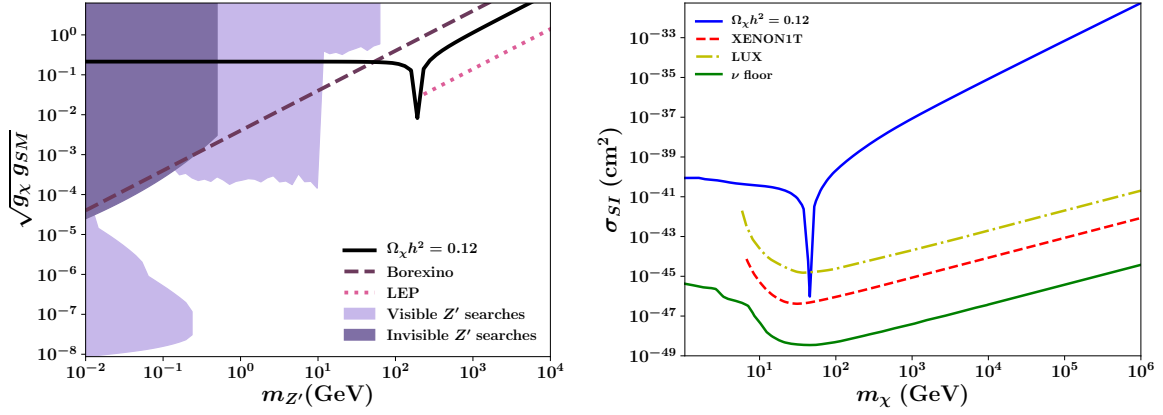


Figure 7. Left frame: Constraints on Dirac dark matter that is coupled to a Z' with couplings to SM leptons, for the case of $m_\chi = 100$ GeV and $g_\chi/g_{SM} = 1$. The regions above the dotted and dashed curves are excluded by LEP and Borexino, respectively. These constraints exclude the entire range of masses in this scenario, except for a window near and slightly below resonance. Right frame: The spin-independent elastic scattering cross section with nuclei in the same model, for the case of $m_{Z'} = 100$ GeV and $g_\chi/g_{SM} = 1$. Current direct detection experiments exclude the range of models shown for all values of m_χ above the threshold for XENON1T, LUX and PandaX-II.

Dirac Dark Matter, Couplings to First Generation Leptons

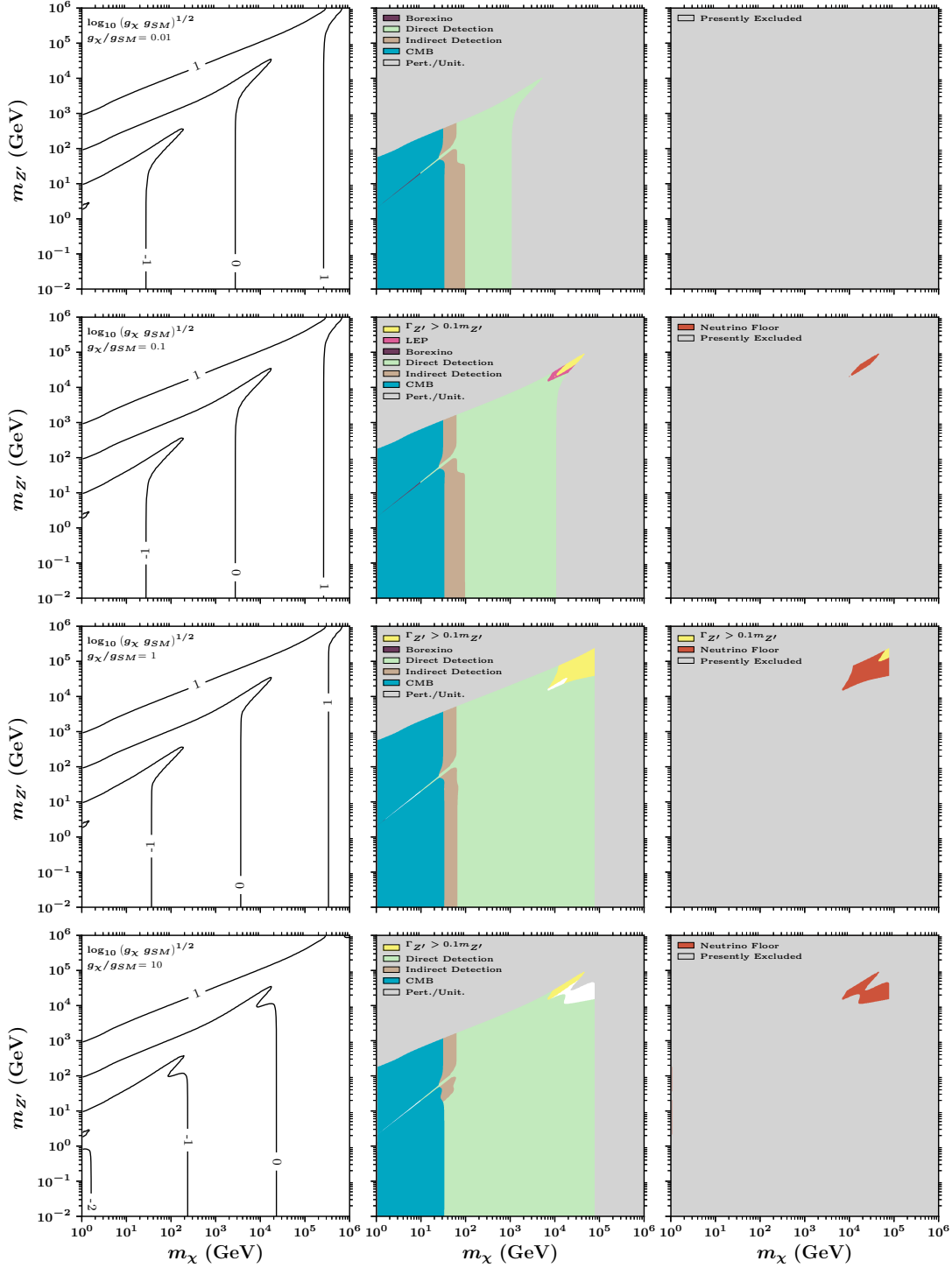


Figure 8. As in previous figures, but for the case of Dirac dark matter that is coupled to a Z' with couplings only to first generation leptons. Again we find that the combined constraints from the cosmic microwave background, direct detection and indirect detection rule out the overwhelming majority of the parameter space shown.

Dirac Dark Matter, Couplings to Third Generation Leptons

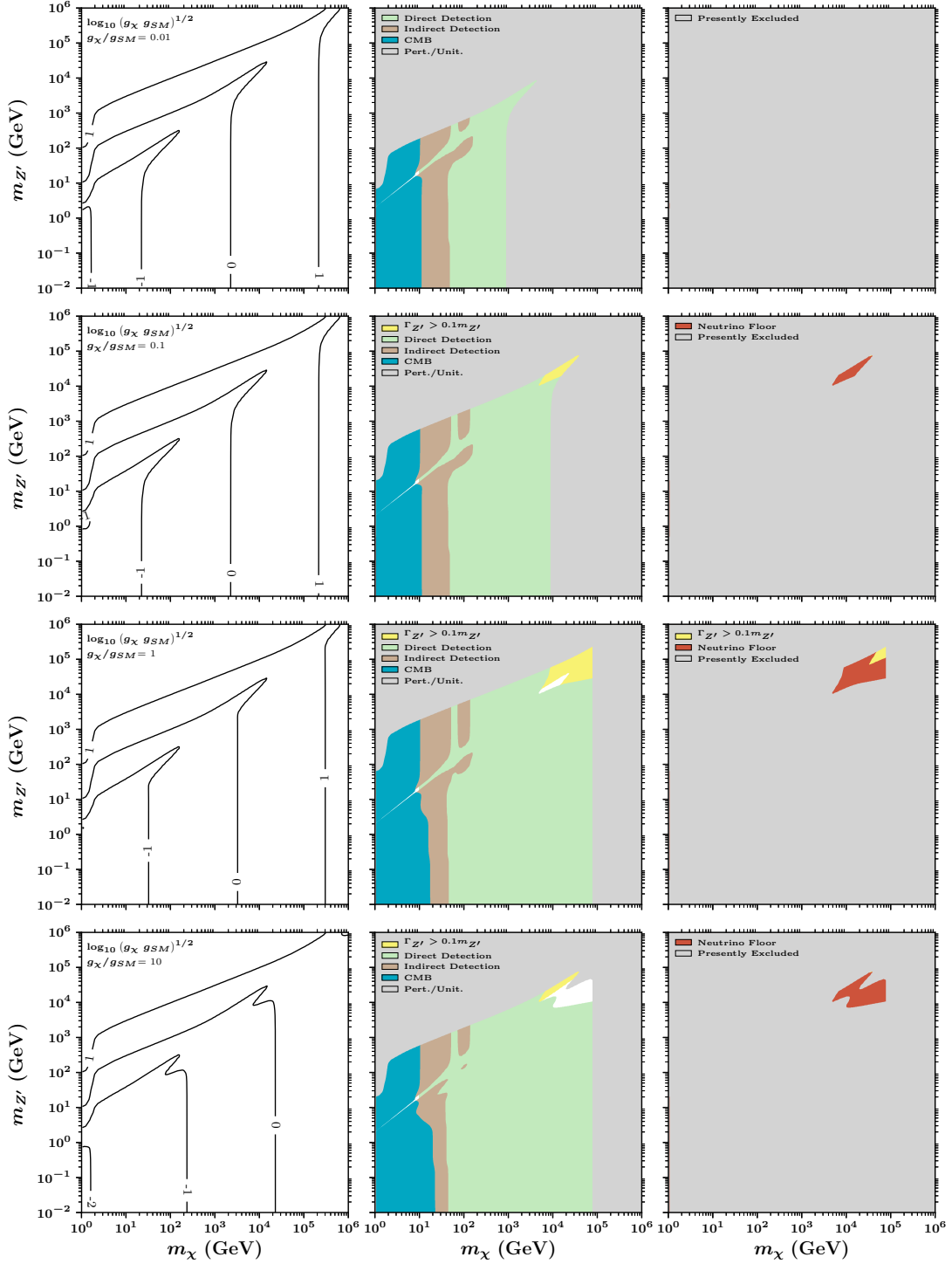


Figure 9. As in previous figures, but for the case of Dirac dark matter that is coupled to a Z' with couplings only to third generation leptons. Again we find that the combined constraints from the cosmic microwave background, direct detection and indirect detection rule out the overwhelming majority of the parameter space shown.

4.2 Majorana Dark Matter

In the previous subsection, we showed that the constraints on Dirac, Z' mediated dark matter leave this class of models strongly constrained across a wide range of the parameter space. In fact, such scenarios are already all but ruled out, and will be fully explored by future direct detection experiments. These constraints are much less restrictive, however, in the case of Majorana dark matter. This is true for two main reasons. First, Majorana dark matter annihilates through p -wave amplitudes, and is thus suppressed at low velocities, reducing the sensitivity of CMB measurements and indirect searches. For this reason, we present our results in this section for dark matter masses down to 10 MeV, below which the measurements of the primordial light element abundances exclude the parameter space. Second, the elastic scattering cross section of Majorana dark matter with nuclei is suppressed by two powers of velocity or momentum, reducing the sensitivity of direct detection experiments by a factor of approximately $\sim 10^{-64}$.

4.2.1 Couplings to Quarks

In Fig. 10, we show our results for the case of Majorana dark matter with a Z' that couples equally to all SM quarks. In this case, constraints from direct detection, colliders and fixed target experiments exclude significant portions of the parameter space, although substantial regions remain viable (in particular for the case of $g_\chi \gtrsim g_{\text{SM}}$). In the right frames of this figure, we see that future direct detection experiments are projected to probe a significant fraction of the remaining parameter space in this model. Even with an array of experiments that reach the neutrino floor, however, some of this parameter space will remain unexplored.

In Fig. 11, we further explore this class of models across specific slices of parameter space. For the case of $m_\chi = 100$ GeV and $g_\chi/g_{\text{SM}} = 1$, searches for light Z' bosons (as characterized using DarkCast [189]) exclude Z' masses below ~ 0.4 GeV, while dijet searches at ATLAS and CMS exclude some regions of parameter space with larger values of $m_{Z'}$. In the right frame, we see that for $m_{Z'} = 100$ GeV and $g_\chi/g_{\text{SM}} = 1$, direct detection experiments current exclude dark matter with masses between $\sim 12 - 33$ GeV and $\sim 54 - 640$ GeV (although future direct detection experiment will explore a much wider range of masses).

In Figs. 12 and 13, we show the results for the case of Majorana dark matter that is coupled to a Z' with couplings only to first or third generation quarks, respectively. Large portions of the parameter space have been (and will be) tested for models in which $g_{\text{SM}} \gtrsim g_\chi$. On the other hand, when the SM coupling is suppressed, large portions of parameter space will likely remain unexplored for some time. In the third generation case, we have again blocked out in red the region of parameter space corresponding to $m_\pi < m_\chi < m_b, m_{Z'}$ where dark matter annihilation occurs through loops to light quarks (or mesons) and leptons.

⁴We note that because of this suppression, loop effects could in principle become important. This effect seems only to be relevant however for a narrow range of low mass WIMPs [231], and thus we neglect this effect in the computations that follow.

Majorana Dark Matter, Couplings to all Quarks

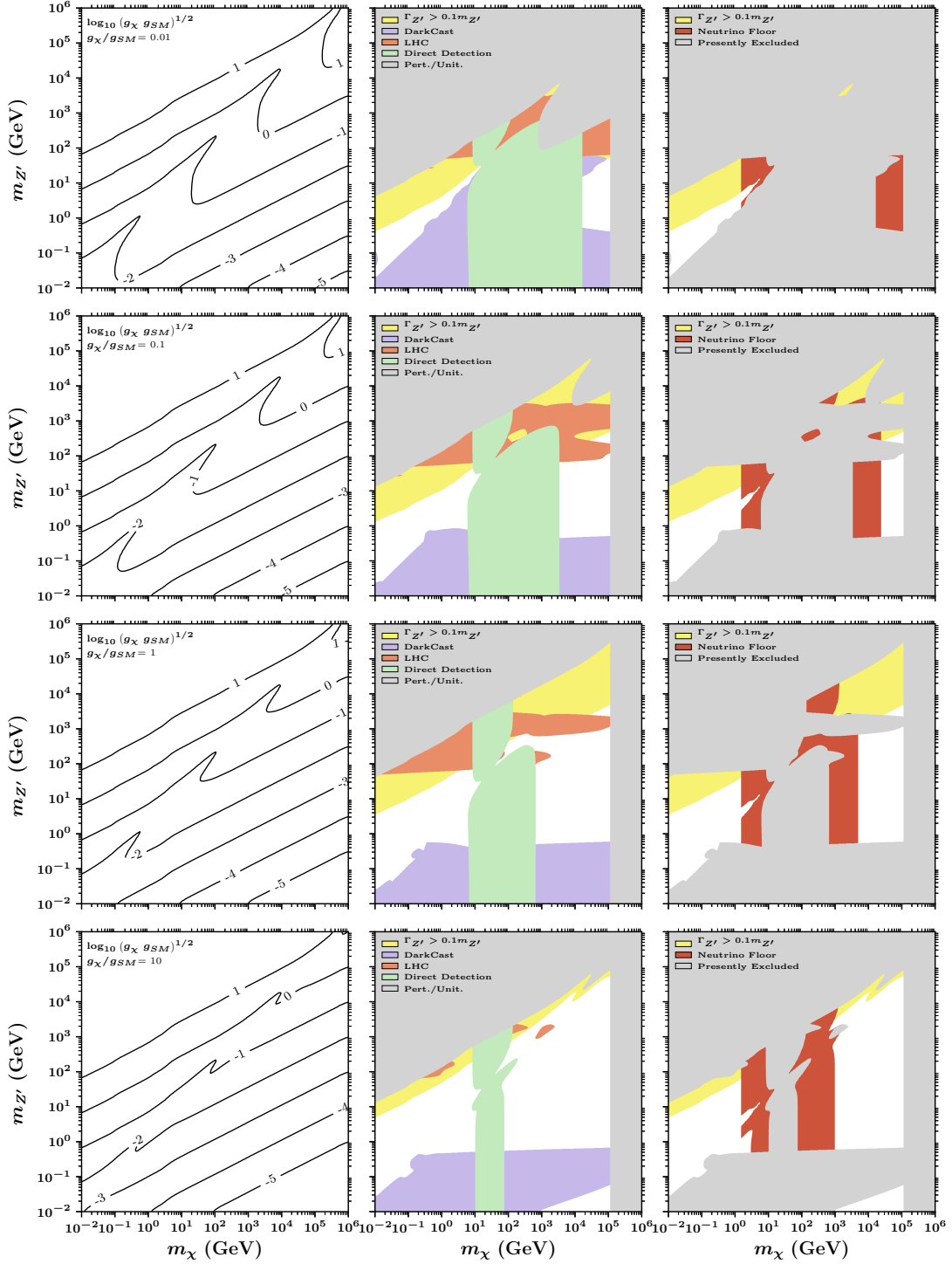


Figure 10. As in previous figures, but for the case of Majorana dark matter that is coupled to a Z' with couplings to all SM quarks. Although the combined constraints from direct detection, colliders and fixed target experiments exclude significant portions of the parameter space, substantial regions remain viable. Future direct detection experiments are projected to be sensitive to much of the remaining parameter space.

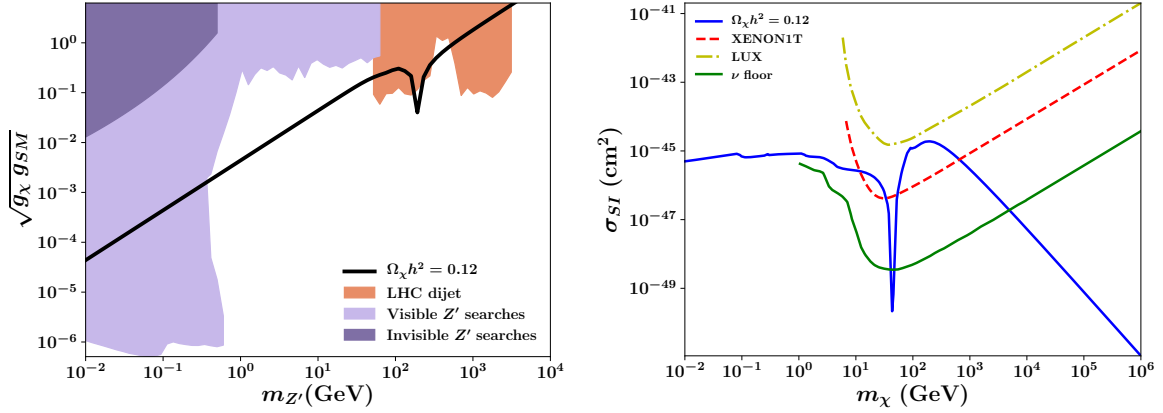


Figure 11. Left Frame: Constraints on Majorana dark matter that is coupled to a Z' with couplings to all SM quarks, for the case of $m_\chi = 100$ GeV and $g_\chi/g_{\text{SM}} = 1$. Searches for light Z' bosons [189] exclude Z' masses below ~ 0.4 GeV, while dijet searches at ATLAS and CMS exclude some regions of parameter space with larger values of $m_{Z'}$. Right frame: The spin-independent elastic scattering cross section with nuclei in the same model, for the case of $m_{Z'} = 100$ GeV and $g_\chi/g_{\text{SM}} = 1$. Current direct detection experiments exclude dark matter with masses between $\sim 10 - 30$ GeV and $\sim 50 - 600$ GeV, and future direct detection experiment will explore a significantly wider range of masses.

4.2.2 Couplings to Leptons

Lastly, we consider the case of Majorana dark matter with a Z' that couples to SM leptons. Among this class of models, Z' searches at LEP, Borexino, and at lower energy colliders and fixed target experiments provide the most powerful constraints. In scenarios with couplings to all SM leptons (see Figs. 14 and 15) or couplings to first generation leptons (Fig. 16), these constraints exclude much of the parameter space, except that with $g_\chi \gtrsim g_{\text{SM}}$, for which this model remains largely unconstrained at high to intermediate dark matter masses. Interestingly, in such models, the loop suppressed direct detection interactions can dominate over the tree level contribution, given that the latter is q^2 and v^2 suppressed while the former is not. Future direct detection experiments will have only a modest impact on the parameter space of this model. In a scenario in which the Z' couples only to third generation leptons, the constraints from Z' become substantially less restrictive, as shown in Fig. 17. This is because such a Z' can be produced in e^+e^- collisions only through loops, and final states including electrons and muons are often easier to identify and reconstruct than those featuring tau leptons.

Majorana Dark Matter, Couplings to First Generation Quarks

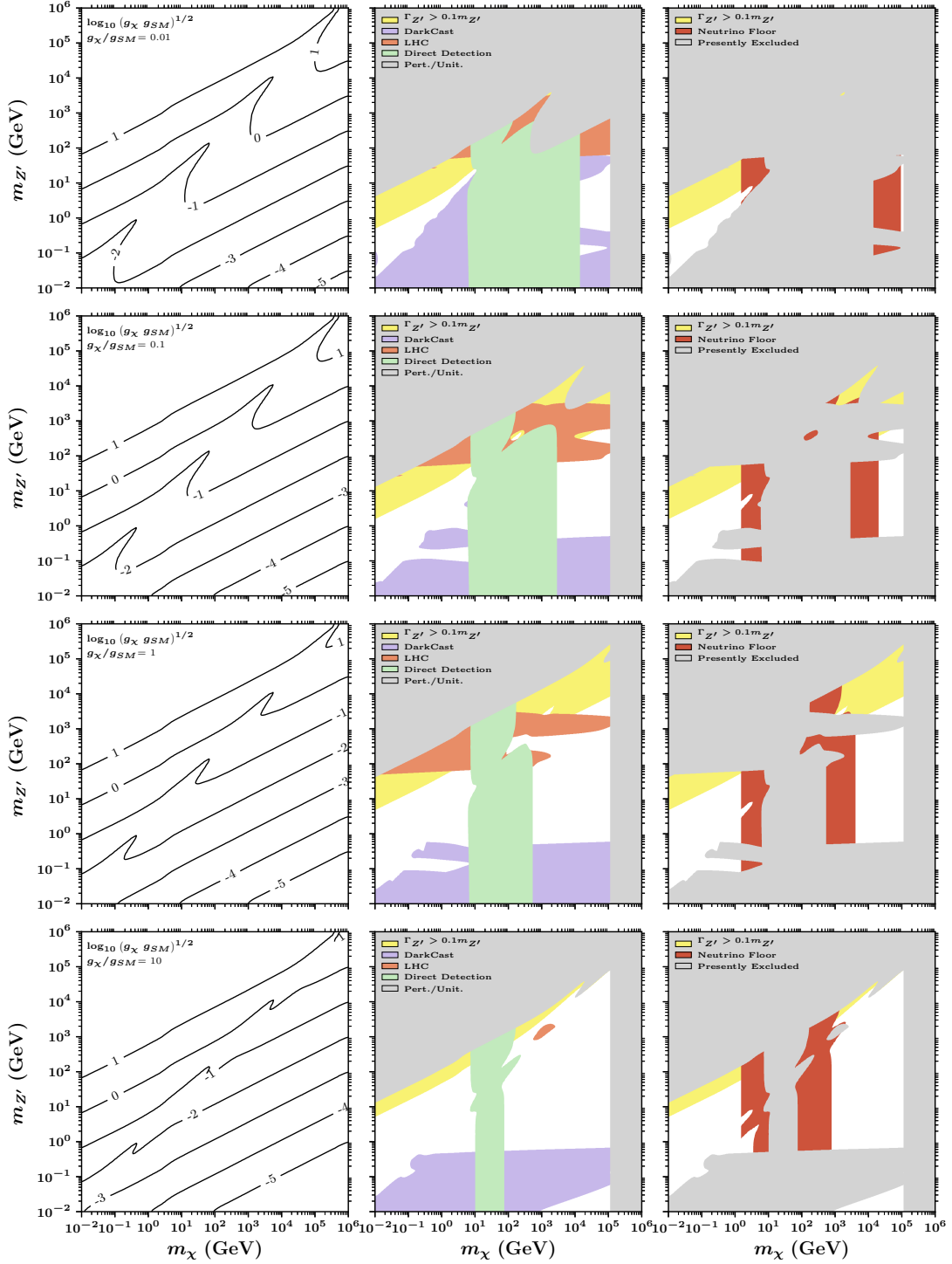


Figure 12. As in previous figures, but for the case of Majorana dark matter that is coupled to a Z' with couplings only to first generation quarks. Although the combined constraints from direct detection, colliders and fixed target experiments exclude significant portions of the parameter space, substantial regions remain viable. Future direct detection experiments are projected to be sensitive to much of the remaining parameter space.

Majorana Dark Matter, Couplings to Third Generation Quarks

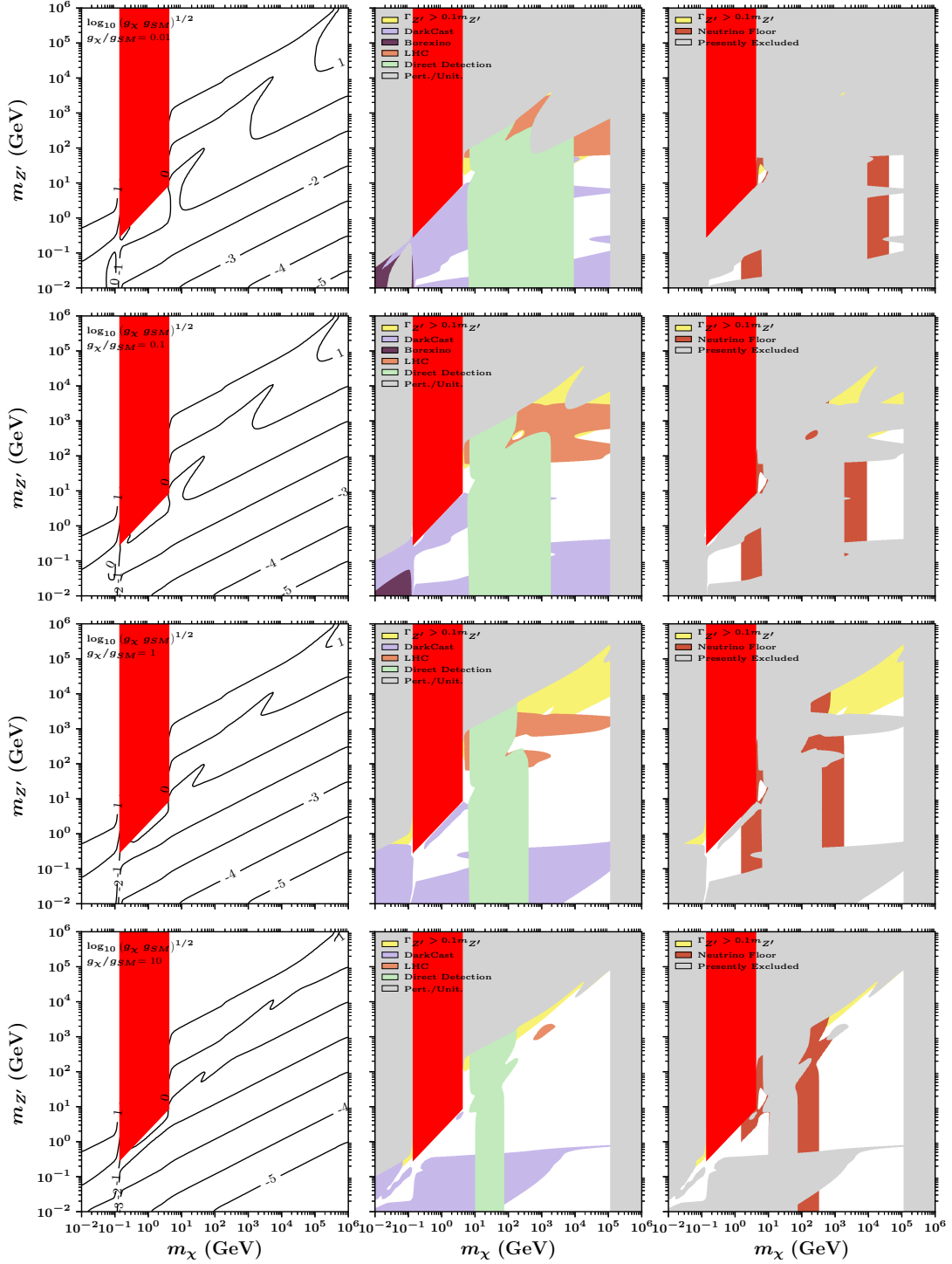


Figure 13. As in previous figures, but for the case of Majorana dark matter that is coupled to a Z' with couplings only to third generation quarks. Although the combined constraints from direct detection, colliders and fixed target experiments exclude significant portions of the parameter space, substantial regions remain viable. Future direct detection experiments are projected to be sensitive to much of the remaining parameter space. In the red regions, annihilations produce a variety of hadronic final states.

Majorana Dark Matter, Couplings to all Leptons

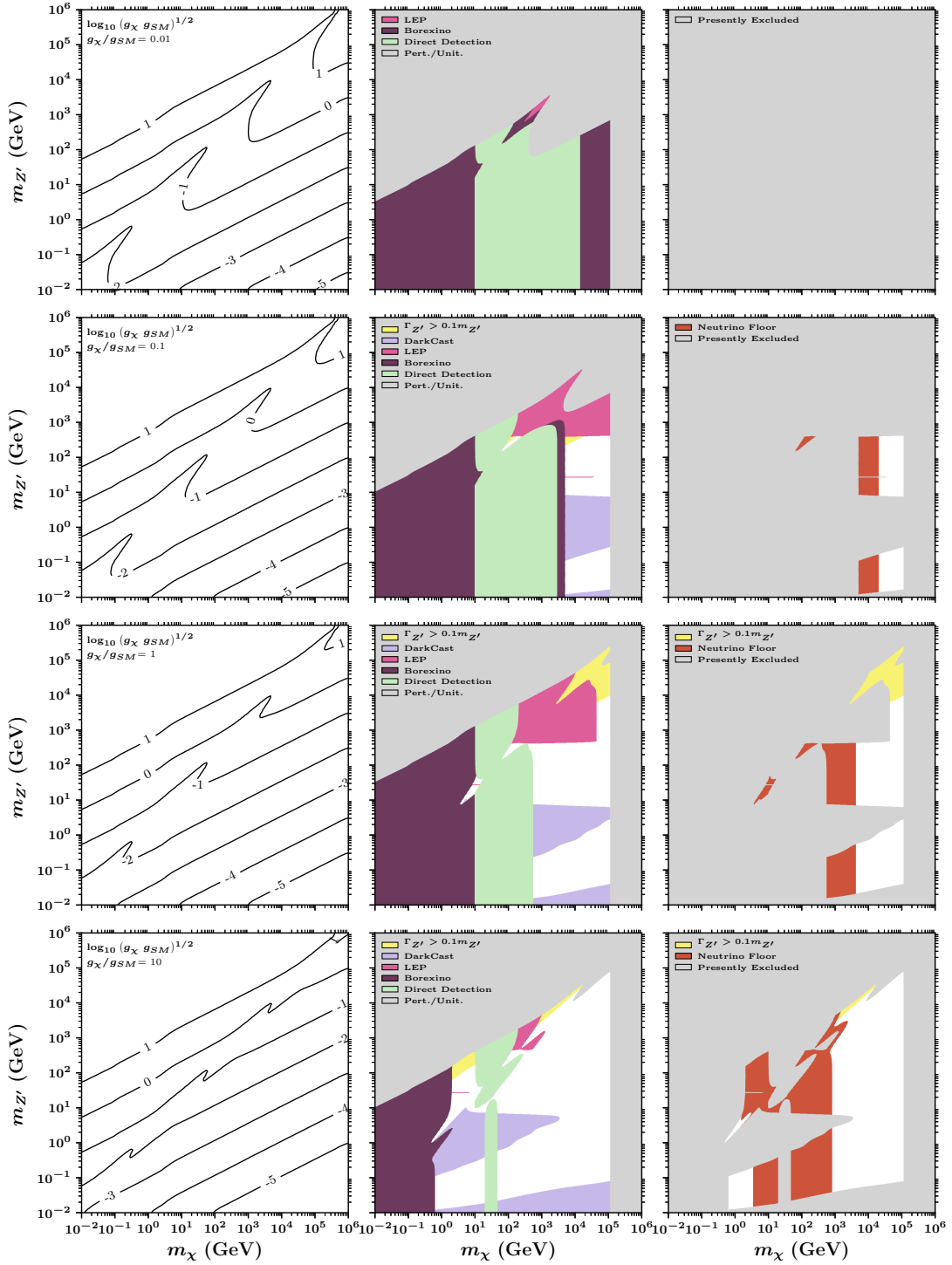


Figure 14. As in previous figures, but for the case of Majorana dark matter that is coupled to a Z' with couplings to all SM leptons. Among this class of models, Z' searches at Borexino, LEP, and lower energy collider and fixed target experiments provide the most powerful constraints.

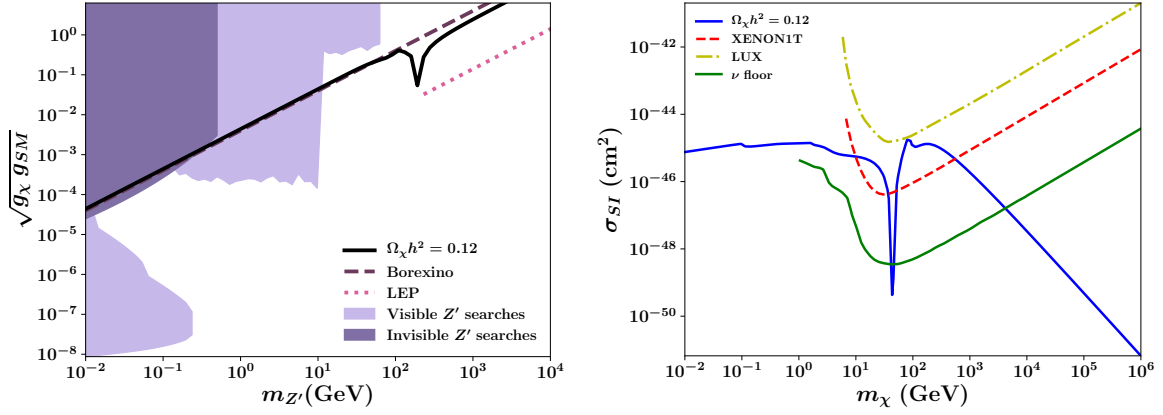


Figure 15. Left Frame: Constraints on Majorana dark matter that is coupled to a Z' with couplings to all SM leptons, for the case of $m_\chi = 100$ GeV and $g_\chi/g_{SM} = 1$. The regions above the dotted and dashed curves are excluded by LEP and Borexino, respectively. Searches for light Z' bosons [189] and constraints from LEP and Borexino exclude most of the parameter space shown. Right frame: The spin-independent elastic scattering cross section with nuclei in the same model, for the case of $m_{Z'} = 100$ GeV and $g_\chi/g_{SM} = 1$. Current direct detection experiments exclude dark matter with masses between $\sim 10 - 40$ GeV and $\sim 50 - 500$ GeV, and future direct detection experiment will explore a significantly wider range of masses.

Majorana Dark Matter, Couplings to First Generation Leptons

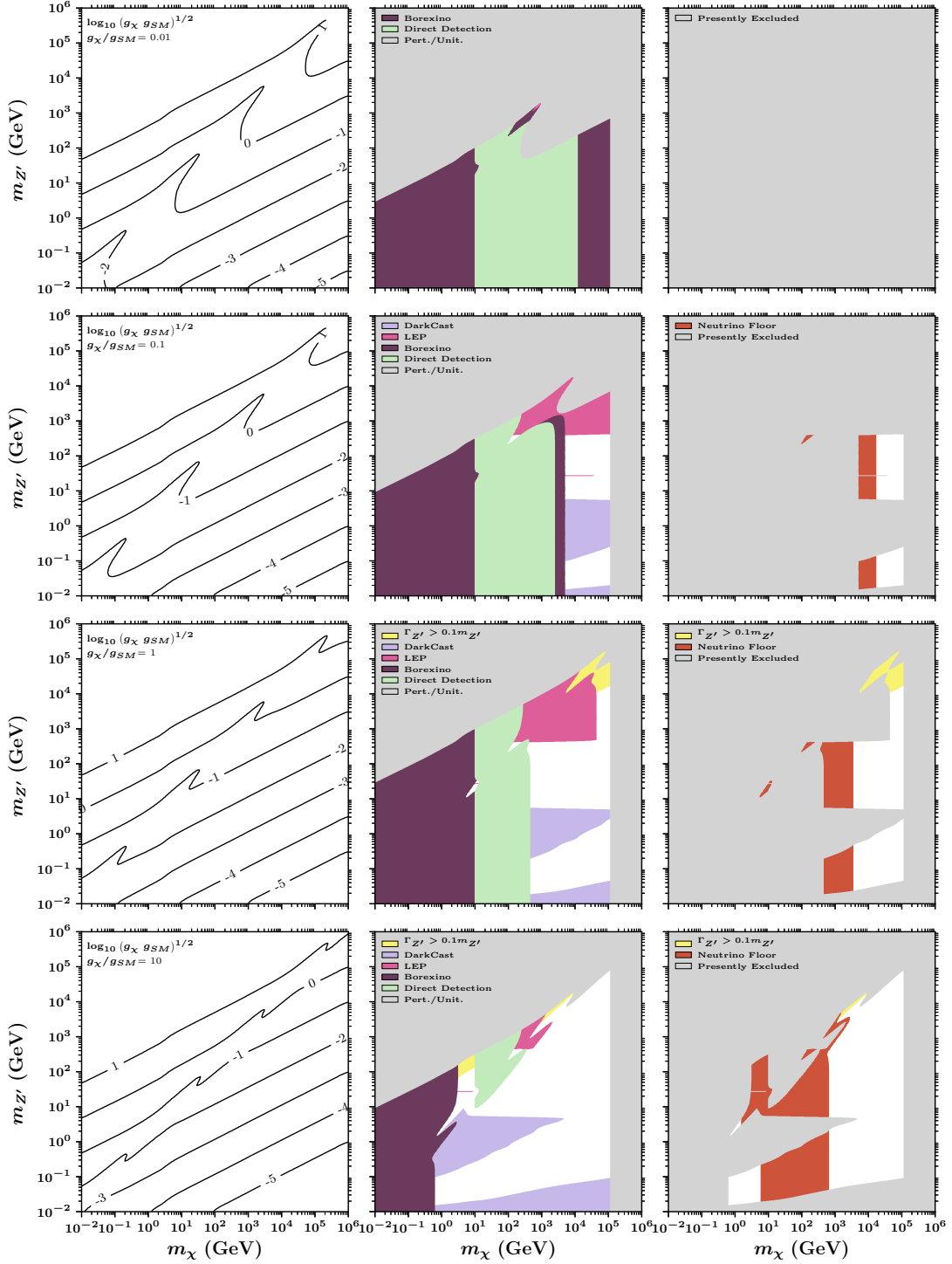


Figure 16. As in previous figures, but for the case of Majorana dark matter that is coupled to a Z' with couplings only to first generation leptons. Among this class of models, Z' searches at Borexino, LEP, and lower energy collider and fixed target experiments provide the most powerful constraints.

Majorana Dark Matter, Couplings to Third Generation Leptons

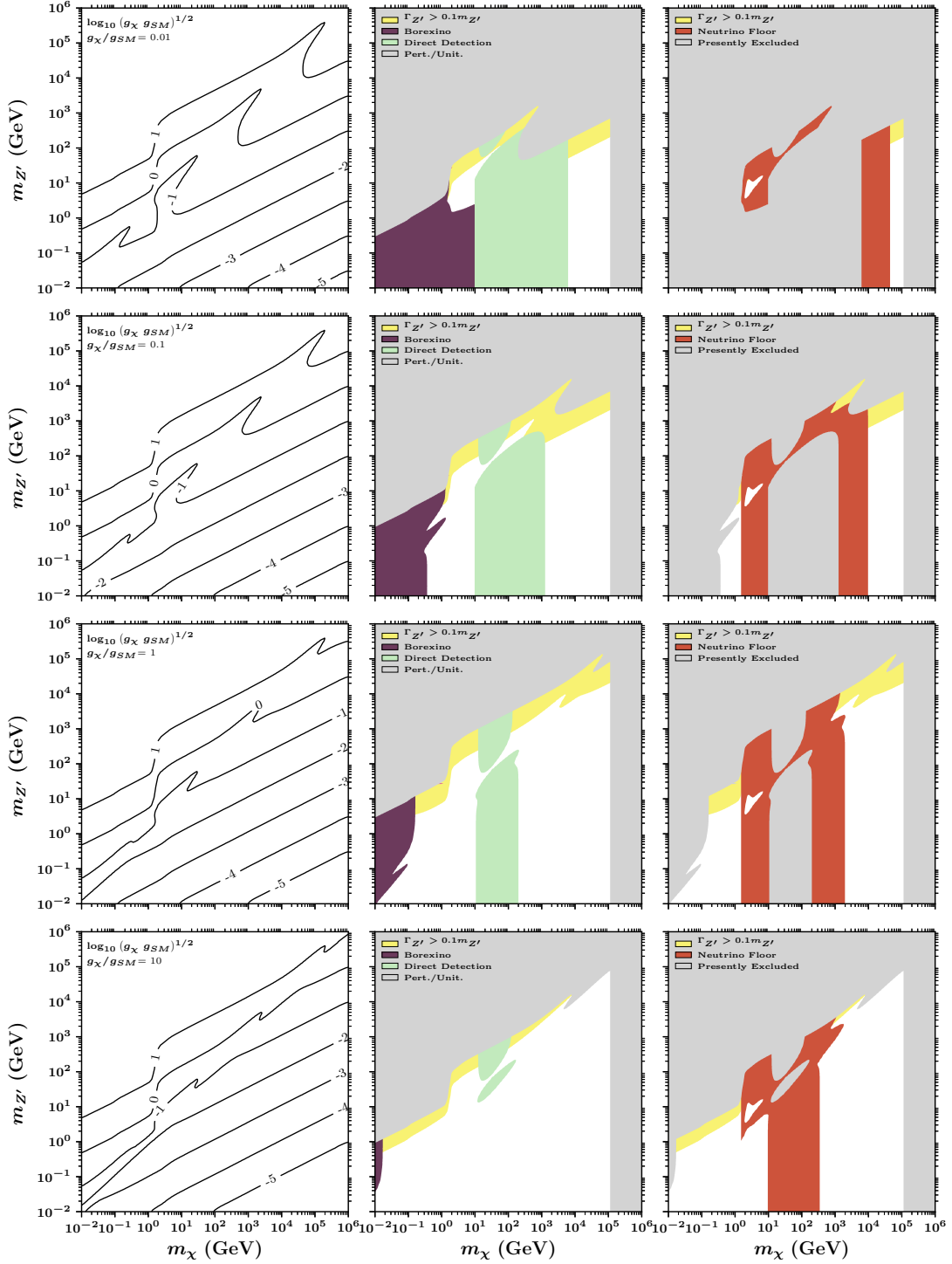


Figure 17. As in previous figures, but for the case of Majorana dark matter that is coupled to a Z' with couplings only to third generation leptons. This is the least constrained class of models among those considered in this study.

5 Caveats and Theoretical Considerations

5.1 Models With an Axial Z'

Throughout this study, we have restricted our attention to models in which the Z' possesses only vectorial couplings to SM fermions. In a more generalized approach, one might also consider the possibility of non-zero axial couplings. Such generalizations generally impact the prospects for direct and indirect detection most strongly, with relatively little impact on the constraints from colliders or fixed target experiments, or on the determination of the thermal relic abundance. Regarding direct detection, adopting a purely axial coupling will lead to a spin-dependent interaction, which is suppressed relative to the spin-independent case a factor of $\sim A^2$, but that is still much larger than those found in typical Majorana models (as considered in Sec. 4.2). From the perspective of indirect detection, the low-velocity annihilation cross section is chirality suppressed in this case (*i.e.* modified by a factor of m_f^2/m_χ^2), yielding similar indirect detection constraints as those found in Sec. 4.2. The phenomenology of an axially coupled dark matter candidate can thus be intuited from the constraints provided in this study.

Theoretically, however, a Z' with purely axial couplings to SM fermions is somewhat difficult to motivate. Although a Z' will couple in a purely axial way to the dark matter if it is a Majorana fermion, the same cannot be said of SM fermions. In Ref. [113] (see also [114]), the authors attempted to motivate purely axial anomaly-free models, but found that such models typically require a large number of new particles with large charge assignments. In order for these new particles to avoid experimental constraints, it is most natural to shift the characteristic mass scale of the new sector to be at or above the TeV scale, typically requiring $\mathcal{O}(1)$ gauge couplings in order to produce the correct relic abundance. The presence of a large gauge coupling and large charges implies that the running will be strong, leading Landau poles to appear at lower scales. Rather than including a new ad-hoc $U(1)$ symmetry (as done in Ref. [113]), one could instead attempt to generate purely axial couplings using a more involved symmetry breaking pattern. For example, within the context of $SO(10)$ [84, 86, 232] it is possible to arrange for a $U(1)_R \times U(1)_{B-L}$ symmetry that is unbroken at relatively low energy scales ($\Lambda \sim \text{TeV}$), and that subsequently breaks to $U(1)_Y$. The gauge boson associated with this symmetry could potentially have purely axial couplings with some SM fermions provided that the gauge couplings of g_{B-L} and g_R are equal (which is not generically expected to be the case). However, since the $U(1)_R$ charges of the SM up and down quarks are flipped, it is not possible in this scenario to generate purely axial interactions to either protons or neutrons, and therefore direct detection constraints will still be very restrictive (see also, Refs. [233–237]).

5.2 UV Complete Models

The models considered in this study are intended to provide an adequate description of the relevant phenomenology, and do not necessarily represent a UV complete description of the underlying theory. More specifically, the gauge invariance of such a theory requires the cancellation of all anomalies arising from triangle diagrams with gauge bosons as external lines. In most cases, this requires the introduction of new chiral fermions, known as exotics [238, 239]. The requirement of perturbativity implies that these particles must be lighter than approximately $m_f \lesssim 5.4 \text{ TeV} \times (m_{Z'}/100 \text{ GeV})(0.1/g_{Z'})(1/q_\varphi)$, where q_φ is the charge of the Higgs field associated with the breaking of the $U(1)'$. Such particles are constrained by the LHC and LEP [240], in particular in the case of small values of $m_{Z'}$ or a large coupling. The triangle diagrams involving exotic fermions can also induce scattering processes that scale like $(E/m_{Z'})^2$, leading to stringent constraints on scenarios with a light Z' [241, 242].

Additionally, the Z_2 symmetry we have imposed by hand in order to stabilize the dark matter particle is rather arbitrary from a theoretical perspective. Many well-motivated models, however, have discrete symmetries that are a result of the symmetry breaking structure of the new gauge symmetry, or by the particle content that is needed in order to cancel anomalies (see, for example, Refs. [110–115, 243]). Scenarios in which Z_2 symmetries arise naturally often involve dark matter particles with masses above the TeV scale.

6 Implications for the WIMP Paradigm

In this section, we will attempt to summarize and synthesize the results of this study, in an effort to more broadly evaluate the status of the WIMP paradigm. At some level, we acknowledge that this goal is perhaps overly ambitious. The WIMP paradigm includes a vast range of models, and the collection of Z' mediated scenarios considered here only begins to scratch the surface of these possibilities. That being said, this collection of models provides us with a fairly representative sample of WIMP models, and we contend that the results of this study can help to illuminate the status of the WIMP paradigm in the presence of the current constraints and projected sensitivity of direct detection, indirect detection and accelerator experiments.

Broadly speaking, our goal here will be to quantitatively determine the extent to which experiments have probed Z' mediated WIMP dark matter. This question is of course to some extent ill-defined, as someone who wholeheartedly believes that dark matter is a ~ 10 TeV neutralino might arrive at the conclusion that $\sim 0\%$ of the dark matter parameter space has been tested, while another convinced dark matter is particle with mass ~ 10 GeV having s-wave annihilations might conclude dark matter has been fully ruled out. This sentiment is a direct consequence of the individuals' prior beliefs, suggesting the question we hope to address here is best framed in the context of a Bayesian analysis. Following this intuition, for each choice of Majorana or Dirac dark matter, charge assignments, and the value of g_χ/g_{SM} , we proceed by defining a model space given by $\Theta = \{m_{Z'}, m_\chi\}$, fixing the couplings using the ratio (as defined in the model) and the relic density, with each mass in Θ bounded from above by perturbativity, unitarity, and $\Gamma_{Z'} < 0.1 m_{Z'}$, and below by successful BBN (approximated here by $m_\chi, m_{Z'} > 10$ MeV) (see Secs. 3.1 and 3.2). The posterior probability given a set of observations, X , is then given by the following:

$$P(\Theta|X) = \frac{P(X|\Theta)P(\Theta)}{P(X)}, \quad (6.1)$$

where $P(X)$ is the Bayesian evidence, given by $\int d\Theta P(X|\Theta) P(\Theta)$, and $P(X|\Theta)$ is the likelihood. At points in parameter space that are not ruled out by the data, the value of $P(X|\Theta)$ is proportional to the volume of the parameter space that yields the measured dark matter abundance, $P(X|\theta) \propto (\partial\Omega_\chi/\partial\log_{10}(g_\chi g_{\text{SM}}))^{-1}$. $P(\Theta)$ is the prior on the parameters and is given by the product of priors on each parameter, $P(\Theta) = P(m_{Z'}) \times P(m_\chi) \times P(g_\chi)$.

An inescapable limitation of any Bayesian analysis is the necessary reliance on intrinsically subjective priors, which can introduce biases and otherwise impact the conclusions of a study. With this in mind, we will adopt three different sets of priors, allowing the reader to weigh them as they deem appropriate. In the first case, we adopt a log-flat prior on both m_χ and $m_{Z'}$. While this choice may be attractive to some for its theoretical neutrality, others could be motivated by considerations such as the electroweak hierarchy problem, leading them to instead focus on scenarios that feature masses near the electroweak scale. With this in mind, our second set of priors features log-normal distributions for $m_{Z'}$ and m_χ , centered around the mass of the SM Higgs boson ($m_h = 125.1$ GeV [244]) and with a one-sigma width of one order of magnitude. Lastly, one might expect gauge couplings to generically

Dirac Dark Matter Model		Prior					
Z' Couples To	g_χ/g_{SM}	Log-Flat		$m_\chi, m_{Z'} \sim \mathcal{O}(m_h)$		$g_\chi, g_{\text{SM}} \sim \mathcal{O}(0.1)$	
		P_{current}	P_{future}	P_{current}	P_{future}	P_{current}	P_{future}
All Quarks	0.01	0.00	0.00	0.00	0.00	0.00	0.00
	0.1	0.00	0.00	0.00	0.00	0.00	0.00
	1.0	0.00	0.00	0.00	0.00	0.00	0.00
	10.0	0.02	0.00	0.02	0.00	0.01	0.00
1st Gen. Quarks	0.01	0.00	0.00	0.00	0.00	0.00	0.00
	0.1	0.00	0.00	0.00	0.00	0.00	0.00
	1.0	0.00	0.00	0.00	0.00	0.00	0.00
	10.0	0.01	0.00	0.01	0.00	0.01	0.00
3rd Gen. Quarks	0.01	0.00	0.00	0.00	0.00	0.00	0.00
	0.1	0.00	0.00	0.00	0.00	0.00	0.00
	1.0	0.00	0.00	0.00	0.00	0.00	0.00
	10.0	0.01	0.00	0.01	0.00	0.01	0.00
All Leptons	0.01	0.00	0.00	0.00	0.00	0.00	0.00
	0.1	0.00	0.00	0.00	0.00	0.00	0.00
	1.0	0.00	0.00	0.00	0.00	0.00	0.00
	10.0	0.02	0.00	0.02	0.00	0.02	0.00
1st Gen. Leptons	0.01	0.00	0.00	0.00	0.00	0.00	0.00
	0.1	0.00	0.00	0.00	0.00	0.00	0.00
	1.0	0.00	0.00	0.00	0.00	0.00	0.00
	10.0	0.01	0.00	0.01	0.00	0.02	0.00
3rd Gen. Leptons	0.01	0.00	0.00	0.00	0.00	0.00	0.00
	0.1	0.00	0.00	0.00	0.00	0.00	0.00
	1.0	0.00	0.00	0.00	0.00	0.00	0.00
	10.0	0.01	0.00	0.01	0.00	0.02	0.00

Table 2. The current probabilities (P_{current}) and the projected probabilities in lieu of any detection by an array of neutrino-floor direct detection experiments (P_{future}), for the case of Dirac, Z' mediated dark matter. We present results corresponding to three sets of Bayesian priors, as described in the text. In this case, the vast majority of the parameter space is already ruled out, and the little remaining viable parameter space will be tested by upcoming direct detection experiments.

possess values near $\mathcal{O}(0.1)$. With this in mind, we adopt in our third case priors on $(m_\chi, m_{Z'})$ such that masses requiring abnormally small couplings are deemed as ‘less favorable’ – specifically, after computing the relic couplings for a particular point in parameter space, the prior is given by a log-normal distribution in each coupling g_χ and g_{SM} , centered about 0.1 and with a one-sigma width of one dex, *i.e.*

$$P(m_\chi, m_{Z'}) = \frac{1}{\sqrt{2\pi}g_\chi g_{\text{SM}}} e^{-\frac{(\log_{10}(g_\chi)-0.1)^2}{2} - \frac{(\log_{10}(g_{\text{SM}})-0.1)^2}{2}}, \quad (6.2)$$

where the functional dependence of g_χ and g_{SM} on m_χ and $m_{Z'}$ is understood implicitly.

As mentioned, we would like to determine the fraction of parameter space within each model which to-date has been ‘ruled out’, defined here to mean that for a particular choice of m_χ and $m_{Z'}$ experimental observations constrain this candidate (at the CLs defined in Sec. 3) from accounting for the entirety of the dark matter. To this end, for each model and choice of prior, we define the ratio of

Majorana Dark Matter Model		Prior					
Z' Couples To	g_χ/g_{SM}	Log-Flat		$m_\chi, m_{Z'} \sim \mathcal{O}(m_h)$		$g_\chi, g_{\text{SM}} \sim \mathcal{O}(0.1)$	
		P_{current}	P_{future}	P_{current}	P_{future}	P_{current}	P_{future}
All Quarks	0.01	0.13	0.06	0.07	0.01	0.11	0.08
	0.1	0.27	0.18	0.23	0.05	0.45	0.29
	1.0	0.37	0.27	0.40	0.10	0.64	0.44
	10.0	0.43	0.33	0.73	0.27	0.76	0.61
1st Gen. Quarks	0.01	0.15	0.08	0.07	0.01	0.13	0.09
	0.1	0.32	0.21	0.22	0.05	0.45	0.30
	1.0	0.40	0.29	0.44	0.12	0.69	0.47
	10.0	0.43	0.34	0.71	0.29	0.73	0.60
3rd Gen. Quarks	0.01	0.19	0.10	0.11	0.04	0.17	0.15
	0.1	0.29	0.20	0.22	0.08	0.48	0.41
	1.0	0.42	0.31	0.54	0.20	0.75	0.55
	10.0	0.52	0.45	0.70	0.44	0.70	0.59
All Leptons	0.01	0.00	0.00	0.00	0.00	0.00	0.00
	0.1	0.16	0.09	0.08	0.02	0.14	0.08
	1.0	0.33	0.21	0.42	0.09	0.44	0.22
	10.0	0.54	0.34	0.83	0.30	0.54	0.38
1st Gen. Leptons	0.01	0.00	0.00	0.00	0.00	0.00	0.00
	0.1	0.17	0.11	0.08	0.03	0.15	0.09
	1.0	0.33	0.22	0.43	0.11	0.41	0.23
	10.0	0.53	0.33	0.84	0.32	0.47	0.34
3rd Gen. Leptons	0.01	0.25	0.07	0.33	0.03	0.24	0.04
	0.1	0.50	0.27	0.36	0.06	0.37	0.17
	1.0	0.69	0.44	0.72	0.18	0.64	0.39
	10.0	0.81	0.61	0.94	0.42	0.70	0.53

Table 3. As in Table 2, but for the case of Majorana, Z' mediated dark matter. With the exception of those models with large couplings to first generation leptons, Z' mediated Majorana dark matter models tend to feature current probabilities in the range of $\mathcal{O}(0.1 - 0.8)$, with prospects for significant improvement from upcoming direct detection experiments.

the Bayesian evidence computed using current experimental constraints to the Bayesian evidence in the absence of any constraint, *i.e.*

$$P_{\text{current}} = \frac{\int d\Theta P(X_{\text{current}}|\Theta) P(\Theta)}{\int d\Theta P(X_{\text{pre-bounds}}|\Theta) P(\Theta)}. \quad (6.3)$$

At first glance it may not be obvious why P_{current} , which is not a well-defined Bayesian statistic, should be thought of as a probability related to the fractional parameter space excluded by current experiments. To understand the significance of P_{current} in terms of well-defined Bayesian quantities, we will consider Bayes' factor B , defined by the ratio of the Bayesian evidence in two competing models. Specifically, we will consider comparing the Bayes' factor between one of the models defined here, and an alternative dark matter model, which we will call model Y (this could *e.g.* be axions, primordial black holes, fuzzy dark matter, etc.). Note that in general, a Bayes' factor $B \sim 1$ shows no model preference, while a large/small value indicates preference for the model in the numerator/denominator.

Now imagine further that no experiments to-date have tested model Y – that is to say, that the Bayesian evidence for model Y is the same today as it was circa 1970. In this case, P_{current} is nothing more than the ratio of the Bayes’ factor today to the value prior to WIMP experimental data, *i.e.*

$$P_{\text{current}} = \frac{B_{\text{current}}}{B_{\text{pre-bounds}}} = \frac{\int d\Theta P(X_{\text{current}}|\Theta) P(\Theta)}{\int d\Theta P(X_{\text{pre-bounds}}|\Theta) P(\Theta)}. \quad (6.4)$$

Suppose that for a given model $B_{\text{pre-bounds}} \sim 10$, and the value of P_{current} is found here to be ~ 0.01 ; in this case, one should conclude that a model which was once viewed as quite favorable relative to model Y , should today be thought of as less favorable. Clearly, the asymptotic behavior of $P_{\text{current}} \rightarrow 1$ ($P_{\text{current}} \rightarrow 0$) coincides with the desired limit that current experimental observations have not probed (or entirely probed) the model of interest.

The definition of Eq. (6.3) can be easily generalized to determine the probability P_{future} of excluding a particular model by the time direct detection experiments reach the neutrino floor. These results are computed using a personalized code and tabulated in Tables 2 and 3, for the case of Dirac and Majorana dark matter, respectively. In the case of Z' mediated Dirac dark matter, the vast majority of the parameter space is already ruled out ($P_{\text{current}} \lesssim 0.02$), regardless of which of these three priors we adopt. In the Majorana case, however, substantial portions of the parameter space remain viable, with P_{current} typically falling in the range of 10% to 80% in the case of log-flat priors. An exception to this are those Majorana models in which the Z' couples significantly to first generation leptons, which are more significantly constrained. Future direct detection experiments are projected in most cases to explore between 20% and 80% of the currently viable parameter space, depending on the scenario considered and which priors are adopted.

7 Discussion and Summary

Although WIMPs have long been viewed as among the most well-motivated classes of dark matter candidates, this paradigm has come to be seen as less attractive in the light of recent experimental constraints. In this study, we set out to explore and, to some degree, quantify the extent to which this reaction is warranted. To this end, we focused on the case of models in which the dark matter annihilates through a new gauge boson, Z' . While certainly not an exhaustive examination of all possible WIMP scenarios, this does provide us with a representative subset of models that we can use to consider the status of the WIMP paradigm.

In the course of this study, we have considered a wide range of scenarios featuring different charge assignments, masses, and couplings, as well as dark matter candidates that are either Dirac or Majorana fermions. We have then determined in each case the fraction of the initially viable parameter space that has been ruled out by existing experiments, as well as the fraction that is projected to be within the reach of future direct detection experiments (with sensitivity near the neutrino floor, as discussed in Sec. 3.6). As these results depend on the Bayesian priors that we adopt on the parameter space, we consider three different sets of priors (see Sec. 6) and allow the reader to weigh them as they see fit.

Some of the main results of our analysis include:

- In the case of Dirac dark matter, the vast majority of the parameter space is already ruled out by a combination of constraints from direct and indirect detection experiments, as well as observations of the cosmic microwave background (the probabilities are $\lesssim 2\%$ for each choice of priors, as shown in Table 2). The small regions that are not currently excluded are projected to be within the reach of upcoming direct detection experiments.

- In the case of Majorana dark matter and a Z' that is coupled to quarks, the current constraints are significant, but less restrictive. Across the range of charge assignments and coupling ratios considered, we find probabilities that fall between 4% and 76% (see Table 3). These models are most significantly constrained by direct detection experiments, the LHC, and a series of lower energy accelerator experiments.
- Scenarios featuring Majorana dark matter and a Z' with substantial couplings to first generation leptons are strongly constrained. In particular, measurements from LEP, Borexino, and lower energy accelerator experiments strongly restrict this class of models.
- We project that future direct detection experiments (with sensitivity near the neutrino floor) will in most cases be sensitive to between 20% and 80% of the currently viable parameter space, depending on which scenario is considered and the priors that are adopted. This provides significant motivation for the next generation of direct detection experiments.
- Scenarios in which the Z' couples more strongly to the dark matter than to SM particles are often much less stringently constrained, although future direct detection experiments will explore much of this parameter space.

Throughout this study, we have defined WIMPs as stable particles that were in equilibrium in the early universe, and that annihilated into SM particles in order to yield a thermal relic abundance equal to the measured cosmological dark matter density. Across much of the parameter space, the determination of the thermal relic abundance depends on the product of the mediator’s couplings to the dark matter and to the SM final states, $\Omega_\chi h^2 \propto (g_\chi g_{\text{SM}})^{-2}$. In the case of $g_\chi \gg g_{\text{SM}}$, however, the dark matter could annihilate directly into $Z'Z'$ (if kinematically allowed, $m_\chi \gtrsim m_{Z'}$), leading to a very different phenomenological picture. In particular, such hidden sector scenarios are less easily tested with direct detection experiments, or at the LHC and other accelerators [41–46, 48–56]. While the null results of such experiments have provided additional motivation for this class of dark matter models, we do not consider them to lie within the boundaries of the WIMP paradigm and thus did not explore them in this study (limiting $g_\chi \leq 10 g_{\text{SM}}$).

Acknowledgments

The authors thank Andrew Fowlie for pointing out some misleading language used in Sec. 6. CB is supported by the US National Science Foundation Graduate Research Fellowship under grants number DGE-1144082 and DGE-1746045. ME is supported by the European Research Council under the European Union’s Horizon 2020 program (ERC Grant Agreement No 648680 DARKHORIZONS). This manuscript has been authored by Fermi Research Alliance, LLC under Contract No. DE-AC02-07CH11359 with the U.S. Department of Energy, Office of High Energy Physics. SW is supported by the Spanish grant FPA2017-85985-P of the MINECO, and by the European Union’s Horizon 2020 research and innovation program under the Marie Skłodowska-Curie grant agreements No. 690575 and 674896.

References

- [1] T. Lin, *TASI lectures on dark matter models and direct detection*, [1904.07915](#).
- [2] D. Hooper, *TASI Lectures on Indirect Searches For Dark Matter*, [1812.02029](#).

- [3] J. M. Cline, *TASI Lectures on Early Universe Cosmology: Inflation, Baryogenesis and Dark Matter*, [1807.08749](#).
- [4] XENON collaboration, E. Aprile et al., *Dark Matter Search Results from a One Ton-Year Exposure of XENON1T*, *Phys. Rev. Lett.* **121** (2018) 111302 [[1805.12562](#)].
- [5] LUX collaboration, D. S. Akerib et al., *Results from a search for dark matter in the complete LUX exposure*, *Phys. Rev. Lett.* **118** (2017) 021303 [[1608.07648](#)].
- [6] PANDAX-II collaboration, X. Cui et al., *Dark Matter Results From 54-Ton-Day Exposure of PandaX-II Experiment*, *Phys. Rev. Lett.* **119** (2017) 181302 [[1708.06917](#)].
- [7] XENON collaboration, E. Aprile et al., *Constraining the spin-dependent WIMP-nucleon cross sections with XENON1T*, *Phys. Rev. Lett.* **122** (2019) 141301 [[1902.03234](#)].
- [8] LUX collaboration, D. S. Akerib et al., *Limits on spin-dependent WIMP-nucleon cross section obtained from the complete LUX exposure*, *Phys. Rev. Lett.* **118** (2017) 251302 [[1705.03380](#)].
- [9] CMS collaboration, A. M. Sirunyan et al., *Search for dark matter particles produced in association with a top quark pair at $\sqrt{s} = 13$ TeV*, *Phys. Rev. Lett.* **122** (2019) 011803 [[1807.06522](#)].
- [10] CMS collaboration, A. M. Sirunyan et al., *Search for narrow and broad dijet resonances in proton-proton collisions at $\sqrt{s} = 13$ TeV and constraints on dark matter mediators and other new particles*, *JHEP* **08** (2018) 130 [[1806.00843](#)].
- [11] CMS collaboration, A. M. Sirunyan et al., *Search for dark matter produced in association with a Higgs boson decaying to $\gamma\gamma$ or $\tau^+\tau^-$ at $\sqrt{s} = 13$ TeV*, *JHEP* **09** (2018) 046 [[1806.04771](#)].
- [12] CMS collaboration, A. M. Sirunyan et al., *Search for new physics in dijet angular distributions using proton-proton collisions at $\sqrt{s} = 13$ TeV and constraints on dark matter and other models*, *Eur. Phys. J. C* **78** (2018) 789 [[1803.08030](#)].
- [13] CMS collaboration, A. M. Sirunyan et al., *Search for dark matter in events with energetic, hadronically decaying top quarks and missing transverse momentum at $\sqrt{s} = 13$ TeV*, *JHEP* **06** (2018) 027 [[1801.08427](#)].
- [14] CMS collaboration, A. M. Sirunyan et al., *Search for top squarks and dark matter particles in opposite-charge dilepton final states at $\sqrt{s} = 13$ TeV*, *Phys. Rev.* **D97** (2018) 032009 [[1711.00752](#)].
- [15] ATLAS collaboration, M. Aaboud et al., *Search for dark matter in events with a hadronically decaying vector boson and missing transverse momentum in pp collisions at $\sqrt{s} = 13$ TeV with the ATLAS detector*, *JHEP* **10** (2018) 180 [[1807.11471](#)].
- [16] ATLAS collaboration, M. Aaboud et al., *Search for dark matter and other new phenomena in events with an energetic jet and large missing transverse momentum using the ATLAS detector*, *JHEP* **01** (2018) 126 [[1711.03301](#)].
- [17] ATLAS collaboration, M. Aaboud et al., *Search for dark matter produced in association with bottom or top quarks in $\sqrt{s} = 13$ TeV pp collisions with the ATLAS detector*, *Eur. Phys. J. C* **78** (2018) 18 [[1710.11412](#)].
- [18] ATLAS collaboration, M. Aaboud et al., *Search for an invisibly decaying Higgs boson or dark matter candidates produced in association with a Z boson in pp collisions at $\sqrt{s} = 13$ TeV with the ATLAS detector*, *Phys. Lett.* **B776** (2018) 318 [[1708.09624](#)].
- [19] ATLAS collaboration, M. Aaboud et al., *Search for Dark Matter Produced in Association with a Higgs Boson Decaying to $b\bar{b}$ using 36 fb^{-1} of pp collisions at $\sqrt{s} = 13$ TeV with the ATLAS Detector*, *Phys. Rev. Lett.* **119** (2017) 181804 [[1707.01302](#)].

- [20] T. Daylan, D. P. Finkbeiner, D. Hooper, T. Linden, S. K. N. Portillo, N. L. Rodd et al., *The characterization of the gamma-ray signal from the central Milky Way: A case for annihilating dark matter*, *Phys. Dark Univ.* **12** (2016) 1 [[1402.6703](#)].
- [21] F. Calore, I. Cholis and C. Weniger, *Background model systematics for the Fermi GeV excess*, *JCAP* **1503** (2015) 038 [[1409.0042](#)].
- [22] L. Goodenough and D. Hooper, *Possible Evidence For Dark Matter Annihilation In The Inner Milky Way From The Fermi Gamma Ray Space Telescope*, [0910.2998](#).
- [23] D. Hooper and L. Goodenough, *Dark Matter Annihilation in The Galactic Center As Seen by the Fermi Gamma Ray Space Telescope*, *Phys. Lett.* **B697** (2011) 412 [[1010.2752](#)].
- [24] D. Hooper and T. Linden, *On The Origin Of The Gamma Rays From The Galactic Center*, *Phys. Rev.* **D84** (2011) 123005 [[1110.0006](#)].
- [25] K. N. Abazajian and M. Kaplinghat, *Detection of a Gamma-Ray Source in the Galactic Center Consistent with Extended Emission from Dark Matter Annihilation and Concentrated Astrophysical Emission*, *Phys. Rev.* **D86** (2012) 083511 [[1207.6047](#)].
- [26] D. Hooper and T. R. Slatyer, *Two Emission Mechanisms in the Fermi Bubbles: A Possible Signal of Annihilating Dark Matter*, *Phys. Dark Univ.* **2** (2013) 118 [[1302.6589](#)].
- [27] FERMI-LAT collaboration, M. Ajello et al., *Fermi-LAT Observations of High-Energy γ -Ray Emission Toward the Galactic Center*, *Astrophys. J.* **819** (2016) 44 [[1511.02938](#)].
- [28] R. K. Leane and T. R. Slatyer, *Dark Matter Strikes Back at the Galactic Center*, [1904.08430](#).
- [29] I. Cholis, T. Linden and D. Hooper, *A Robust Excess in the Cosmic-Ray Antiproton Spectrum: Implications for Annihilating Dark Matter*, *Phys. Rev.* **D99** (2019) 103026 [[1903.02549](#)].
- [30] A. Cuoco, J. Heisig, L. Klamt, M. Korsmeier and M. Krämer, *Scrutinizing the evidence for dark matter in cosmic-ray antiprotons*, *Phys. Rev.* **D99** (2019) 103014 [[1903.01472](#)].
- [31] A. Cuoco, M. Krämer and M. Korsmeier, *Novel Dark Matter Constraints from Antiprotons in Light of AMS-02*, *Phys. Rev. Lett.* **118** (2017) 191102 [[1610.03071](#)].
- [32] M.-Y. Cui, Q. Yuan, Y.-L. S. Tsai and Y.-Z. Fan, *Possible dark matter annihilation signal in the AMS-02 antiproton data*, *Phys. Rev. Lett.* **118** (2017) 191101 [[1610.03840](#)].
- [33] G. Bertone and M. P. Tait, Tim, *A new era in the search for dark matter*, *Nature* **562** (2018) 51 [[1810.01668](#)].
- [34] P. Agrawal, G. Marques-Tavares and W. Xue, *Opening up the QCD axion window*, *JHEP* **03** (2018) 049 [[1708.05008](#)].
- [35] P. Agrawal, J. Fan, M. Reece and L.-T. Wang, *Experimental Targets for Photon Couplings of the QCD Axion*, *JHEP* **02** (2018) 006 [[1709.06085](#)].
- [36] N. Blinov, M. J. Dolan, P. Draper and J. Kozaczuk, *Dark Matter Targets for Axion-like Particle Searches*, [1905.06952](#).
- [37] P. Arias, D. Cadamuro, M. Goodsell, J. Jaeckel, J. Redondo and A. Ringwald, *WISPy Cold Dark Matter*, *JCAP* **1206** (2012) 013 [[1201.5902](#)].
- [38] D. J. E. Marsh, *Axion Cosmology*, *Phys. Rept.* **643** (2016) 1 [[1510.07633](#)].
- [39] P. W. Graham, I. G. Irastorza, S. K. Lamoreaux, A. Lindner and K. A. van Bibber, *Experimental Searches for the Axion and Axion-Like Particles*, *Ann. Rev. Nucl. Part. Sci.* **65** (2015) 485 [[1602.00039](#)].

- [40] I. G. Irastorza and J. Redondo, *New experimental approaches in the search for axion-like particles*, *Prog. Part. Nucl. Phys.* **102** (2018) 89 [[1801.08127](#)].
- [41] M. Pospelov, A. Ritz and M. B. Voloshin, *Secluded WIMP Dark Matter*, *Phys. Lett.* **B662** (2008) 53 [[0711.4866](#)].
- [42] N. Arkani-Hamed, D. P. Finkbeiner, T. R. Slatyer and N. Weiner, *A Theory of Dark Matter*, *Phys. Rev.* **D79** (2009) 015014 [[0810.0713](#)].
- [43] M. Abdullah, A. DiFranzo, A. Rajaraman, T. M. P. Tait, P. Tanedo and A. M. Wijangco, *Hidden on-shell mediators for the Galactic Center γ -ray excess*, *Phys. Rev.* **D90** (2014) 035004 [[1404.6528](#)].
- [44] A. Berlin, P. Gratia, D. Hooper and S. D. McDermott, *Hidden Sector Dark Matter Models for the Galactic Center Gamma-Ray Excess*, *Phys. Rev.* **D90** (2014) 015032 [[1405.5204](#)].
- [45] A. Martin, J. Shelton and J. Unwin, *Fitting the Galactic Center Gamma-Ray Excess with Cascade Annihilations*, *Phys. Rev.* **D90** (2014) 103513 [[1405.0272](#)].
- [46] D. Hooper, N. Weiner and W. Xue, *Dark Forces and Light Dark Matter*, *Phys. Rev.* **D86** (2012) 056009 [[1206.2929](#)].
- [47] J. M. Cline, G. Dupuis, Z. Liu and W. Xue, *The windows for kinetically mixed Z' -mediated dark matter and the galactic center gamma ray excess*, *JHEP* **08** (2014) 131 [[1405.7691](#)].
- [48] A. Berlin, D. Hooper and G. Krnjaic, *PeV-Scale Dark Matter as a Thermal Relic of a Decoupled Sector*, *Phys. Lett.* **B760** (2016) 106 [[1602.08490](#)].
- [49] A. Berlin, D. Hooper and G. Krnjaic, *Thermal Dark Matter From A Highly Decoupled Sector*, *Phys. Rev.* **D94** (2016) 095019 [[1609.02555](#)].
- [50] J. A. Dror, E. Kuflik and W. H. Ng, *Codecaying Dark Matter*, *Phys. Rev. Lett.* **117** (2016) 211801 [[1607.03110](#)].
- [51] J. A. Dror, E. Kuflik, B. Melcher and S. Watson, *Concentrated dark matter: Enhanced small-scale structure from codecaying dark matter*, *Phys. Rev.* **D97** (2018) 063524 [[1711.04773](#)].
- [52] J. L. Feng, M. Kaplinghat, H. Tu and H.-B. Yu, *Hidden Charged Dark Matter*, *JCAP* **0907** (2009) 004 [[0905.3039](#)].
- [53] C. Cheung, G. Elor, L. J. Hall and P. Kumar, *Origins of Hidden Sector Dark Matter I: Cosmology*, *JHEP* **03** (2011) 042 [[1010.0022](#)].
- [54] X. Chu, T. Hambye and M. H. G. Tytgat, *The Four Basic Ways of Creating Dark Matter Through a Portal*, *JCAP* **1205** (2012) 034 [[1112.0493](#)].
- [55] M. Escudero, N. Rius and V. Sanz, *Sterile Neutrino portal to Dark Matter II: Exact Dark symmetry*, *Eur. Phys. J.* **C77** (2017) 397 [[1607.02373](#)].
- [56] K. M. Zurek, *Asymmetric Dark Matter: Theories, Signatures, and Constraints*, *Phys. Rept.* **537** (2014) 91 [[1308.0338](#)].
- [57] M. Escudero, S. J. Witte and D. Hooper, *Hidden Sector Dark Matter and the Galactic Center Gamma-Ray Excess: A Closer Look*, *JCAP* **1711** (2017) 042 [[1709.07002](#)].
- [58] G. Elor, M. Escudero and A. Nelson, *Baryogenesis and Dark Matter from B Mesons*, *Phys. Rev.* **D99** (2019) 035031 [[1810.00880](#)].
- [59] M. Escudero, A. Berlin, D. Hooper and M.-X. Lin, *Toward (Finally!) Ruling Out Z and Higgs Mediated Dark Matter Models*, *JCAP* **1612** (2016) 029 [[1609.09079](#)].
- [60] G. Arcadi, M. Dutra, P. Ghosh, M. Lindner, Y. Mambrini, M. Pierre et al., *The waning of the WIMP? A review of models, searches, and constraints*, *Eur. Phys. J.* **C78** (2018) 203 [[1703.07364](#)].

- [61] J. Ellis, A. Fowlie, L. Marzola and M. Raidal, *Statistical Analyses of Higgs- and Z-Portal Dark Matter Models*, *Phys. Rev.* **D97** (2018) 115014 [[1711.09912](#)].
- [62] G. B. Gelmini, *Light weakly interacting massive particles*, *Rept. Prog. Phys.* **80** (2017) 082201 [[1612.09137](#)].
- [63] M. Bauer and T. Plehn, *Yet Another Introduction to Dark Matter*, *Lect. Notes Phys.* **959** (2019) pp. [[1705.01987](#)].
- [64] L. Roszkowski, E. M. Sessolo and S. Trojanowski, *WIMP dark matter candidates and searches—current status and future prospects*, *Rept. Prog. Phys.* **81** (2018) 066201 [[1707.06277](#)].
- [65] K. Kowalska and E. M. Sessolo, *The discreet charm of higgsino dark matter - a pocket review*, *Adv. High Energy Phys.* **2018** (2018) 6828560 [[1802.04097](#)].
- [66] K. Agashe, A. Falkowski, I. Low and G. Servant, *KK Parity in Warped Extra Dimension*, *JHEP* **04** (2008) 027 [[0712.2455](#)].
- [67] K. Agashe and G. Servant, *Baryon number in warped GUTs: Model building and (dark matter related) phenomenology*, *JCAP* **0502** (2005) 002 [[hep-ph/0411254](#)].
- [68] K. Agashe and G. Servant, *Warped unification, proton stability and dark matter*, *Phys. Rev. Lett.* **93** (2004) 231805 [[hep-ph/0403143](#)].
- [69] H.-S. Lee, K. T. Matchev and S. Nasri, *Revival of the thermal sneutrino dark matter*, *Phys. Rev.* **D76** (2007) 041302 [[hep-ph/0702223](#)].
- [70] M. R. Buckley, D. Hooper and J. L. Rosner, *A Leptophobic Z' And Dark Matter From Grand Unification*, *Phys. Lett.* **B703** (2011) 343 [[1106.3583](#)].
- [71] M. Buckley, P. Fileviez Perez, D. Hooper and E. Neil, *Dark Forces At The Tevatron*, *Phys. Lett.* **B702** (2011) 256 [[1104.3145](#)].
- [72] G. Belanger, A. Pukhov and G. Servant, *Dirac Neutrino Dark Matter*, *JCAP* **0801** (2008) 009 [[0706.0526](#)].
- [73] T. Hur, H.-S. Lee and S. Nasri, *A Supersymmetric U(1)-prime model with multiple dark matters*, *Phys. Rev.* **D77** (2008) 015008 [[0710.2653](#)].
- [74] L. Delle Rose, S. Khalil, S. J. D. King, C. Marzo, S. Moretti and C. S. Un, *Naturalness and dark matter in the supersymmetric B-L extension of the standard model*, *Phys. Rev.* **D96** (2017) 055004 [[1702.01808](#)].
- [75] L. Delle Rose, S. Khalil, S. J. D. King, S. Kulkarni, C. Marzo, S. Moretti et al., *Sneutrino Dark Matter in the BLSSM*, *JHEP* **07** (2018) 100 [[1712.05232](#)].
- [76] O. Lebedev and Y. Mambrini, *Axial dark matter: The case for an invisible Z'*, *Phys. Lett.* **B734** (2014) 350 [[1403.4837](#)].
- [77] G. Arcadi, Y. Mambrini, M. H. G. Tytgat and B. Zaldivar, *Invisible Z' and dark matter: LHC vs LUX constraints*, *JHEP* **03** (2014) 134 [[1401.0221](#)].
- [78] M. Fairbairn, J. Heal, F. Kahlhoefer and P. Tunney, *Constraints on Z? models from LHC dijet searches and implications for dark matter*, *JHEP* **09** (2016) 018 [[1605.07940](#)].
- [79] E. Dudas, L. Heurtier, Y. Mambrini and B. Zaldivar, *Extra U(1), effective operators, anomalies and dark matter*, *JHEP* **11** (2013) 083 [[1307.0005](#)].
- [80] X. Chu, Y. Mambrini, J. Quevillon and B. Zaldivar, *Thermal and non-thermal production of dark matter via Z'-portal(s)*, *JCAP* **1401** (2014) 034 [[1306.4677](#)].

- [81] Y. Mambrini, *The ZZ' kinetic mixing in the light of the recent direct and indirect dark matter searches*, *JCAP* **1107** (2011) 009 [[1104.4799](#)].
- [82] E. Dudas, Y. Mambrini, S. Pokorski and A. Romagnoni, *(In)visible Z-prime and dark matter*, *JHEP* **08** (2009) 014 [[0904.1745](#)].
- [83] D. Hooper, *Z' mediated dark matter models for the Galactic Center gamma-ray excess*, *Phys. Rev.* **D91** (2015) 035025 [[1411.4079](#)].
- [84] P. Langacker, *The Physics of Heavy Z' Gauge Bosons*, *Rev. Mod. Phys.* **81** (2009) 1199 [[0801.1345](#)].
- [85] D. London and J. L. Rosner, *Extra Gauge Bosons in $E(6)$* , *Phys. Rev.* **D34** (1986) 1530.
- [86] J. L. Hewett and T. G. Rizzo, *Low-Energy Phenomenology of Superstring Inspired $E(6)$ Models*, *Phys. Rept.* **183** (1989) 193.
- [87] V. Braun, Y.-H. He, B. A. Ovrut and T. Pantev, *A Standard model from the $E(8) \times E(8)$ heterotic superstring*, *JHEP* **06** (2005) 039 [[hep-th/0502155](#)].
- [88] G. Cleaver, M. Cvetič, J. R. Espinosa, L. L. Everett, P. Langacker and J. Wang, *Physics implications of flat directions in free fermionic superstring models 1. Mass spectrum and couplings*, *Phys. Rev.* **D59** (1999) 055005 [[hep-ph/9807479](#)].
- [89] C. Coriano, A. E. Faraggi and M. Guzzi, *A Novel string derived Z-prime with stable proton, light-neutrinos and R-parity violation*, *Eur. Phys. J.* **C53** (2008) 421 [[0704.1256](#)].
- [90] A. E. Faraggi and D. V. Nanopoulos, *A SUPERSTRING Z' AT O (1-TeV) ?*, *Mod. Phys. Lett.* **A6** (1991) 61.
- [91] J. Giedt, *Completion of standard model like embeddings*, *Annals Phys.* **289** (2001) 251 [[hep-th/0009104](#)].
- [92] O. Lebedev, H. P. Nilles, S. Raby, S. Ramos-Sanchez, M. Ratz, P. K. S. Vaudrevange et al., *The Heterotic Road to the MSSM with R parity*, *Phys. Rev.* **D77** (2008) 046013 [[0708.2691](#)].
- [93] P. Anastasopoulos, M. Bianchi, E. Dudas and E. Kiritsis, *Anomalies, anomalous $U(1)$'s and generalized Chern-Simons terms*, *JHEP* **11** (2006) 057 [[hep-th/0605225](#)].
- [94] A. E. Faraggi, *Yukawa couplings in superstring derived standard like models*, *Phys. Rev.* **D47** (1993) 5021.
- [95] M. Cvetič, G. Shiu and A. M. Uranga, *Chiral four-dimensional $N=1$ supersymmetric type 2A orientifolds from intersecting D6 branes*, *Nucl. Phys.* **B615** (2001) 3 [[hep-th/0107166](#)].
- [96] C. T. Hill and E. H. Simmons, *Strong dynamics and electroweak symmetry breaking*, *Phys. Rept.* **381** (2003) 235 [[hep-ph/0203079](#)].
- [97] R. S. Chivukula, H.-J. He, J. Howard and E. H. Simmons, *The Structure of electroweak corrections due to extended gauge symmetries*, *Phys. Rev.* **D69** (2004) 015009 [[hep-ph/0307209](#)].
- [98] R. S. Chivukula and E. H. Simmons, *Electroweak limits on nonuniversal Z-prime bosons*, *Phys. Rev.* **D66** (2002) 015006 [[hep-ph/0205064](#)].
- [99] K. Agashe, A. Delgado, M. J. May and R. Sundrum, *$RS1$, custodial isospin and precision tests*, *JHEP* **08** (2003) 050 [[hep-ph/0308036](#)].
- [100] K. Agashe, H. Davoudiasl, S. Gopalakrishna, T. Han, G.-Y. Huang, G. Perez et al., *LHC Signals for Warped Electroweak Neutral Gauge Bosons*, *Phys. Rev.* **D76** (2007) 115015 [[0709.0007](#)].
- [101] M. Carena, A. Delgado, E. Ponton, T. M. P. Tait and C. E. M. Wagner, *Precision electroweak data and unification of couplings in warped extra dimensions*, *Phys. Rev.* **D68** (2003) 035010 [[hep-ph/0305188](#)].

- [102] J. L. Hewett, F. J. Petriello and T. G. Rizzo, *Precision measurements and fermion geography in the Randall-Sundrum model revisited*, *JHEP* **09** (2002) 030 [[hep-ph/0203091](#)].
- [103] N. Arkani-Hamed, A. G. Cohen and H. Georgi, *Electroweak symmetry breaking from dimensional deconstruction*, *Phys. Lett.* **B513** (2001) 232 [[hep-ph/0105239](#)].
- [104] M. Cvetič, D. A. Demir, J. R. Espinosa, L. L. Everett and P. Langacker, *Electroweak breaking and the mu problem in supergravity models with an additional $U(1)$* , *Phys. Rev.* **D56** (1997) 2861 [[hep-ph/9703317](#)].
- [105] P. Langacker, N. Polonsky and J. Wang, *A Low-energy solution to the mu problem in gauge mediation*, *Phys. Rev.* **D60** (1999) 115005 [[hep-ph/9905252](#)].
- [106] N. Arkani-Hamed, A. G. Cohen and H. Georgi, *Anomalies on orbifolds*, *Phys. Lett.* **B516** (2001) 395 [[hep-th/0103135](#)].
- [107] N. Arkani-Hamed, A. G. Cohen, E. Katz, A. E. Nelson, T. Gregoire and J. G. Wacker, *The Minimal moose for a little Higgs*, *JHEP* **08** (2002) 021 [[hep-ph/0206020](#)].
- [108] T. Han, H. E. Logan, B. McElrath and L.-T. Wang, *Phenomenology of the little Higgs model*, *Phys. Rev.* **D67** (2003) 095004 [[hep-ph/0301040](#)].
- [109] M. Perelstein, *Little Higgs models and their phenomenology*, *Prog. Part. Nucl. Phys.* **58** (2007) 247 [[hep-ph/0512128](#)].
- [110] P. Fileviez Perez and M. B. Wise, *Baryon and lepton number as local gauge symmetries*, *Phys. Rev.* **D82** (2010) 011901 [[1002.1754](#)].
- [111] M. Duerr, P. Fileviez Perez and M. B. Wise, *Gauge Theory for Baryon and Lepton Numbers with Leptoquarks*, *Phys. Rev. Lett.* **110** (2013) 231801 [[1304.0576](#)].
- [112] M. Duerr and P. Fileviez Perez, *Theory for Baryon Number and Dark Matter at the LHC*, *Phys. Rev.* **D91** (2015) 095001 [[1409.8165](#)].
- [113] A. Ismail, W.-Y. Keung, K.-H. Tsao and J. Unwin, *Axial vector Z' ? and anomaly cancellation*, *Nucl. Phys.* **B918** (2017) 220 [[1609.02188](#)].
- [114] J. A. Casas, M. Chakraborti and J. Quilis, *UV completion of an axial, leptophobic, Z'* , [1907.11207](#).
- [115] J. Ellis, M. Fairbairn and P. Tunney, *Anomaly-Free Dark Matter Models are not so Simple*, *JHEP* **08** (2017) 053 [[1704.03850](#)].
- [116] J. Ellis, M. Fairbairn and P. Tunney, *Phenomenological Constraints on Anomaly-Free Dark Matter Models*, [1807.02503](#).
- [117] S. Caron, J. A. Casas, J. Quilis and R. Ruiz de Austri, *Anomaly-free Dark Matter with Harmless Direct Detection Constraints*, *JHEP* **12** (2018) 126 [[1807.07921](#)].
- [118] E. Madge and P. Schwaller, *Leptophilic dark matter from gauged lepton number: Phenomenology and gravitational wave signatures*, *JHEP* **02** (2019) 048 [[1809.09110](#)].
- [119] P. Fileviez Perez, E. Golias, R.-H. Li and C. Murgui, *Leptophobic Dark Matter and the Baryon Number Violation Scale*, *Phys. Rev.* **D99** (2019) 035009 [[1810.06646](#)].
- [120] P. Fileviez Pérez, E. Golias, R.-H. Li, C. Murgui and A. D. Plascencia, *On Anomaly-Free Dark Matter Models*, [1904.01017](#).
- [121] S. El Hedri and K. Nordstrom, *Whac-a-constraint with anomaly-free dark matter models*, *SciPost Phys.* **6** (2019) 020 [[1809.02453](#)].
- [122] M. Escudero, S. J. Witte and N. Rius, *The dispirited case of gauged $U(1)_{B-L}$ dark matter*, *JHEP* **08** (2018) 190 [[1806.02823](#)].

- [123] P. Foldenauer, *Light dark matter in a gauged $U(1)_{L_\mu-L_\tau}$ model*, *Phys. Rev.* **D99** (2019) 035007 [[1808.03647](#)].
- [124] E. Bagnaschi et al., *Global Analysis of Dark Matter Simplified Models with Leptophobic Spin-One Mediators using MasterCode*, [1905.00892](#).
- [125] A. Das, S. Goswami, K. N. Vishnudath and T. Nomura, *Constraining a general $U(1)'$ inverse seesaw model from vacuum stability, dark matter and collider*, [1905.00201](#).
- [126] A. Alves, A. Berlin, S. Profumo and F. S. Queiroz, *Dirac-fermionic dark matter in $U(1)_X$ models*, *JHEP* **10** (2015) 076 [[1506.06767](#)].
- [127] F. Kahlhoefer, K. Schmidt-Hoberg, T. Schwetz and S. Vogl, *Implications of unitarity and gauge invariance for simplified dark matter models*, *JHEP* **02** (2016) 016 [[1510.02110](#)].
- [128] M. E. Peskin and T. Takeuchi, *Estimation of oblique electroweak corrections*, *Phys. Rev.* **D46** (1992) 381.
- [129] P. Langacker and M.-x. Luo, *Constraints on additional Z bosons*, *Phys. Rev.* **D45** (1992) 278.
- [130] Y. Umeda, G.-C. Cho and K. Hagiwara, *Constraints on leptophobic Z' models from electroweak experiments*, *Phys. Rev.* **D58** (1998) 115008 [[hep-ph/9805447](#)].
- [131] K. S. Babu, C. F. Kolda and J. March-Russell, *Implications of generalized Z - Z-prime mixing*, *Phys. Rev.* **D57** (1998) 6788 [[hep-ph/9710441](#)].
- [132] B. Holdom, *Two $U(1)$'s and Epsilon Charge Shifts*, *Phys. Lett.* **166B** (1986) 196.
- [133] N. F. Bell, Y. Cai, R. K. Leane and A. D. Medina, *Leptophilic dark matter with Z' interactions*, *Phys. Rev.* **D90** (2014) 035027 [[1407.3001](#)].
- [134] A. A. Andrianov, P. Osland, A. A. Pankov, N. V. Romanenko and J. Sirkka, *On the phenomenology of a Z' coupling only to third family fermions*, *Phys. Rev.* **D58** (1998) 075001 [[hep-ph/9804389](#)].
- [135] C. T. Hill, *Topcolor assisted technicolor*, *Phys. Lett.* **B345** (1995) 483 [[hep-ph/9411426](#)].
- [136] F. del Aguila, G. A. Blair, M. Daniel and G. G. Ross, *Analysis of Neutral Currents in Superstring Inspired Models*, *Nucl. Phys.* **B283** (1987) 50.
- [137] PLANCK collaboration, N. Aghanim et al., *Planck 2018 results. VI. Cosmological parameters*, [1807.06209](#).
- [138] G. Belanger, F. Boudjema, A. Pukhov and A. Semenov, *micromegas 3: A program for calculating dark matter observables*, *Comput. Phys. Commun.* **185** (2014) 960 [[1305.0237](#)].
- [139] C. Boehm, M. J. Dolan and C. McCabe, *A Lower Bound on the Mass of Cold Thermal Dark Matter from Planck*, *JCAP* **1308** (2013) 041 [[1303.6270](#)].
- [140] K. M. Nollett and G. Steigman, *BBN And The CMB Constrain Neutrino Coupled Light WIMPs*, *Phys. Rev.* **D91** (2015) 083505 [[1411.6005](#)].
- [141] M. Escudero, *Neutrino decoupling beyond the Standard Model: CMB constraints on the Dark Matter mass with a fast and precise N_{eff} evaluation*, *JCAP* **1902** (2019) 007 [[1812.05605](#)].
- [142] P. A. Ade, N. Aghanim, M. Arnaud, M. Ashdown, J. Aumont, C. Baccigalupi et al., *Planck 2015 results-xiii. cosmological parameters*, *Astronomy & Astrophysics* **594** (2016) A13 [[1712.01279](#)].
- [143] T. Sjöstrand, S. Ask, J. R. Christiansen, R. Corke, N. Desai, P. Ilten et al., *An Introduction to PYTHIA 8.2*, *Comput. Phys. Commun.* **191** (2015) 159 [[1410.3012](#)].
- [144] T. R. Slatyer, *Indirect dark matter signatures in the cosmic dark ages. I. Generalizing the bound on s-wave dark matter annihilation from Planck results*, *Phys. Rev.* **D93** (2016) 023527 [[1506.03811](#)].

- [145] R. K. Leane, T. R. Slatyer, J. F. Beacom and K. C. Y. Ng, *GeV-scale thermal WIMPs: Not even slightly ruled out*, *Phys. Rev.* **D98** (2018) 023016 [[1805.10305](#)].
- [146] FERMI-LAT, DES collaboration, A. Albert et al., *Searching for Dark Matter Annihilation in Recently Discovered Milky Way Satellites with Fermi-LAT*, *Astrophys. J.* **834** (2017) 110 [[1611.03184](#)].
- [147] AMS collaboration, M. Aguilar et al., *Electron and Positron Fluxes in Primary Cosmic Rays Measured with the Alpha Magnetic Spectrometer on the International Space Station*, *Phys. Rev. Lett.* **113** (2014) 121102.
- [148] AMS collaboration, L. Accardo et al., *High Statistics Measurement of the Positron Fraction in Primary Cosmic Rays of 0.5-500 GeV with the Alpha Magnetic Spectrometer on the International Space Station*, *Phys. Rev. Lett.* **113** (2014) 121101.
- [149] G. Elor, N. L. Rodd, T. R. Slatyer and W. Xue, *Model-Independent Indirect Detection Constraints on Hidden Sector Dark Matter*, *JCAP* **1606** (2016) 024 [[1511.08787](#)].
- [150] G. Elor, N. L. Rodd and T. R. Slatyer, *Multistep cascade annihilations of dark matter and the Galactic Center excess*, *Phys. Rev.* **D91** (2015) 103531 [[1503.01773](#)].
- [151] ATLAS collaboration, M. Aaboud et al., *Search for new phenomena in dijet events using 37 fb⁻¹ of pp collision data collected at $\sqrt{s}=13$ TeV with the ATLAS detector*, *Phys. Rev.* **D96** (2017) 052004 [[1703.09127](#)].
- [152] CMS collaboration, V. Khachatryan et al., *Search for narrow resonances in dijet final states at $\sqrt{s}=8$ TeV with the novel CMS technique of data scouting*, *Phys. Rev. Lett.* **117** (2016) 031802 [[1604.08907](#)].
- [153] CMS collaboration, A. M. Sirunyan et al., *Search for dijet resonances in proton proton collisions at $s=13$ tev and constraints on dark matter and other models*, *Phys. Lett.* **B769** (2017) 520 [[1611.03568](#)].
- [154] CMS collaboration, A. M. Sirunyan et al., *Search for low mass vector resonances decaying into quark-antiquark pairs in proton-proton collisions at $\sqrt{s}=13$ TeV*, *JHEP* **01** (2018) 097 [[1710.00159](#)].
- [155] ATLAS collaboration, G. Aad et al., *Search for new phenomena in the dijet mass distribution using $p-p$ collision data at $\sqrt{s}=8$ TeV with the ATLAS detector*, *Phys. Rev.* **D91** (2015) 052007 [[1407.1376](#)].
- [156] CMS collaboration, V. Khachatryan et al., *Search for resonances and quantum black holes using dijet mass spectra in proton-proton collisions at $\sqrt{s}=8$ TeV*, *Phys. Rev.* **D91** (2015) 052009 [[1501.04198](#)].
- [157] B. A. Dobrescu and F. Yu, *Coupling-Mass Mapping of Dijet Peak Searches*, *Phys. Rev.* **D88** (2013) 035021 [[1306.2629](#)].
- [158] ATLAS collaboration, M. Aaboud et al., *Search for new high-mass phenomena in the dilepton final state using 36 fb⁻¹ of proton-proton collision data at 13 TeV with the ATLAS detector*, *JHEP* **10** (2017) 182 [[1707.02424](#)].
- [159] CMS collaboration, A. M. Sirunyan et al., *Search for high-mass resonances in dilepton final states in proton-proton collisions at $\sqrt{s}=13$ TeV*, *JHEP* **06** (2018) 120 [[1803.06292](#)].
- [160] M. Carena, A. Daleo, B. A. Dobrescu and T. M. P. Tait, *Z' gauge bosons at the Tevatron*, *Phys. Rev.* **D70** (2004) 093009 [[hep-ph/0408098](#)].
- [161] A1 collaboration, H. Merkel et al., *Search at the Mainz Microtron for light massive gauge bosons relevant for the muon $g-2$ anomaly*, *Phys. Rev. Lett.* **112** (2014) 221802 [[1404.5502](#)].
- [162] APEX collaboration, S. Abrahamyan et al., *Search for a new gauge boson in electron-nucleus fixed-target scattering by the APEX experiment*, *Phys. Rev. Lett.* **107** (2011) 191804 [[1108.2750](#)].

- [163] BESIII collaboration, M. Ablikim et al., *Dark Photon Search in the Mass Range Between 1.5 and 3.4 GeV/c²*, *Phys. Lett.* **B774** (2017) 252 [[1705.04265](#)].
- [164] BABAR collaboration, J. P. Lees et al., *Search for a dark photon in e⁺e⁻ collisions at BaBar*, *Phys. Rev. Lett.* **113** (2014) 201801 [[1406.2980](#)].
- [165] CHARM collaboration, F. Bergsma et al., *Search for Axion Like Particle Production in 400-GeV Proton - Copper Interactions*, *Phys. Lett.* **157B** (1985) 458.
- [166] J. D. Bjorken, S. Ecklund, W. R. Nelson, A. Abashian, C. Church, B. Lu et al., *Search for Neutral Metastable Penetrating Particles Produced in the SLAC Beam Dump*, *Phys. Rev.* **D38** (1988) 3375.
- [167] E. M. Riordan et al., *A Search for Short Lived Axions in an Electron Beam Dump Experiment*, *Phys. Rev. Lett.* **59** (1987) 755.
- [168] A. Bross, M. Crisler, S. H. Pordes, J. Volk, S. Errede and J. Wrbanek, *A Search for Short-lived Particles Produced in an Electron Beam Dump*, *Phys. Rev. Lett.* **67** (1991) 2942.
- [169] P. H. Adrian et al., *Search for a Dark Photon in Electro-Produced e⁺e⁻ Pairs with the Heavy Photon Search Experiment at JLab*, [1807.11530](#).
- [170] A. Konaka et al., *Search for Neutral Particles in Electron Beam Dump Experiment*, *Phys. Rev. Lett.* **57** (1986) 659.
- [171] A. Anastasi et al., *Limit on the production of a low-mass vector boson in e⁺e⁻oUγ, Uoe⁺e⁻ with the KLOE experiment*, *Phys. Lett.* **B750** (2015) 633 [[1509.00740](#)].
- [172] KLOE-2 collaboration, A. Anastasi et al., *Limit on the production of a new vector boson in ightrightarrow, U e⁺e⁻π⁺π⁻ with the KLOE experiment*, *Phys. Lett.* **B757** (2016) 356 [[1603.06086](#)].
- [173] KLOE-2 collaboration, A. Anastasi et al., *Combined limit on the production of a light gauge boson decaying into μ⁺μ⁻ and π⁺π⁻*, *Submitted to: Phys. Lett. B* (2018) [[1807.02691](#)].
- [174] KLOE-2 collaboration, D. Babusci et al., *Limit on the production of a light vector gauge boson in phi meson decays with the KLOE detector*, *Phys. Lett.* **B720** (2013) 111 [[1210.3927](#)].
- [175] KLOE-2 collaboration, D. Babusci et al., *Search for light vector boson production in e⁺e⁻ ightrightarrow μ⁺μ⁻γ interactions with the KLOE experiment*, *Phys. Lett.* **B736** (2014) 459 [[1404.7772](#)].
- [176] LHCb collaboration, R. Aaij et al., *Search for Dark Photons Produced in 13 TeV pp Collisions*, *Phys. Rev. Lett.* **120** (2018) 061801 [[1710.02867](#)].
- [177] NA48/2 collaboration, J. R. Batley et al., *Search for the dark photon in π⁰ decays*, *Phys. Lett.* **B746** (2015) 178 [[1504.00607](#)].
- [178] NA64 collaboration, D. Banerjee et al., *Search for a new X(16.7) boson and dark photons in the NA64 experiment at CERN*, [1803.07748](#).
- [179] NOMAD collaboration, P. Astier et al., *Search for heavy neutrinos mixing with tau neutrinos*, *Phys. Lett.* **B506** (2001) 27 [[hep-ex/0101041](#)].
- [180] J. Blumlein et al., *Limits on neutral light scalar and pseudoscalar particles in a proton beam dump experiment*, *Z. Phys.* **C51** (1991) 341.
- [181] J. Blumlein et al., *Limits on the mass of light (pseudo)scalar particles from Bethe-Heitler e+ e- and mu+ mu- pair production in a proton - iron beam dump experiment*, *Int. J. Mod. Phys.* **A7** (1992) 3835.
- [182] M. Davier and H. Nguyen Ngoc, *An Unambiguous Search for a Light Higgs Boson*, *Phys. Lett.* **B229** (1989) 150.
- [183] G. Bernardi et al., *Search for Neutrino Decay*, *Phys. Lett.* **166B** (1986) 479.

- [184] BABAR collaboration, J. P. Lees et al., *Search for Invisible Decays of a Dark Photon Produced in e^+e^- Collisions at BaBar*, *Phys. Rev. Lett.* **119** (2017) 131804 [[1702.03327](#)].
- [185] P. J. Fox, R. Harnik, J. Kopp and Y. Tsai, *LEP Shines Light on Dark Matter*, *Phys. Rev.* **D84** (2011) 014028 [[1103.0240](#)].
- [186] NA64 collaboration, D. Banerjee et al., *Search for invisible decays of sub-GeV dark photons in missing-energy events at the CERN SPS*, *Phys. Rev. Lett.* **118** (2017) 011802 [[1610.02988](#)].
- [187] NA64 collaboration, D. Banerjee et al., *Search for vector mediator of Dark Matter production in invisible decay mode*, *Phys. Rev.* **D97** (2018) 072002 [[1710.00971](#)].
- [188] D. Banerjee et al., *Dark matter search in missing energy events with NA64*, [1906.00176](#).
- [189] P. Ilten, Y. Soreq, M. Williams and W. Xue, *Serendipity in dark photon searches*, *JHEP* **06** (2018) 004 [[1801.04847](#)].
- [190] G. Bellini et al., *Precision measurement of the ^7Be solar neutrino interaction rate in Borexino*, *Phys. Rev. Lett.* **107** (2011) 141302 [[1104.1816](#)].
- [191] R. Harnik, J. Kopp and P. A. N. Machado, *Exploring ν Signals in Dark Matter Detectors*, *JCAP* **1207** (2012) 026 [[1202.6073](#)].
- [192] A. Kamada and H.-B. Yu, *Coherent Propagation of PeV Neutrinos and the Dip in the Neutrino Spectrum at IceCube*, *Phys. Rev.* **D92** (2015) 113004 [[1504.00711](#)].
- [193] J. Billard, L. Strigari and E. Figueroa-Feliciano, *Implication of neutrino backgrounds on the reach of next generation dark matter direct detection experiments*, *Phys. Rev.* **D89** (2014) 023524 [[1307.5458](#)].
- [194] F. Ruppin, J. Billard, E. Figueroa-Feliciano and L. Strigari, *Complementarity of dark matter detectors in light of the neutrino background*, *Phys. Rev.* **D90** (2014) 083510 [[1408.3581](#)].
- [195] W. C. Haxton, R. G. Hamish Robertson and A. M. Serenelli, *Solar Neutrinos: Status and Prospects*, *Ann. Rev. Astron. Astrophys.* **51** (2013) 21 [[1208.5723](#)].
- [196] A. M. Serenelli, W. C. Haxton and C. Pena-Garay, *Solar models with accretion. I. Application to the solar abundance problem*, *Astrophys. J.* **743** (2011) 24 [[1104.1639](#)].
- [197] T. K. Gaisser and M. Honda, *Flux of atmospheric neutrinos*, *Ann. Rev. Nucl. Part. Sci.* **52** (2002) 153 [[hep-ph/0203272](#)].
- [198] S. Horiuchi, J. F. Beacom and E. Dwek, *The Diffuse Supernova Neutrino Background is detectable in Super-Kamiokande*, *Phys. Rev.* **D79** (2009) 083013 [[0812.3157](#)].
- [199] J. F. Beacom, *The Diffuse Supernova Neutrino Background*, *Ann. Rev. Nucl. Part. Sci.* **60** (2010) 439 [[1004.3311](#)].
- [200] N. Raj, V. Takhistov and S. J. Witte, *Pre-Supernova Neutrinos in Large Dark Matter Direct Detection Experiments*, [1905.09283](#).
- [201] S. Chakraborty, P. Bhattacharjee and K. Kar, *Observing supernova neutrino light curve in future dark matter detectors*, *Phys. Rev.* **D89** (2014) 013011 [[1309.4492](#)].
- [202] XMASS collaboration, K. Abe et al., *Detectability of galactic supernova neutrinos coherently scattered on xenon nuclei in XMASS*, *Astropart. Phys.* **89** (2017) 51 [[1604.01218](#)].
- [203] R. F. Lang, C. McCabe, S. Reichard, M. Selvi and I. Tamborra, *Supernova neutrino physics with xenon dark matter detectors: A timely perspective*, *Phys. Rev.* **D94** (2016) 103009 [[1606.09243](#)].
- [204] T. Kozynets, S. Fallows and C. B. Krauss, *Sensitivity of the PICO-500 Bubble Chamber to Supernova Neutrinos Through Coherent Nuclear Elastic Scattering*, *Astropart. Phys.* **105** (2019) 25 [[1806.01417](#)].

- [205] LZ collaboration, D. Khaitan, *Supernova neutrino detection in LZ*, *JINST* **13** (2018) C02024 [[1801.05651](#)].
- [206] F. Reines and C. Cowan Jr, *Detection of the free neutrino*, *Physical Review* **92** (1953) 830.
- [207] F. Reines, C. Cowan Jr, F. Harrison, A. McGuire and H. Kruse, *Detection of the free antineutrino*, *Physical Review* **117** (1960) 159.
- [208] A. C. Hayes and P. Vogel, *Reactor Neutrino Spectra*, *Ann. Rev. Nucl. Part. Sci.* **66** (2016) 219 [[1605.02047](#)].
- [209] T. Araki et al., *Experimental investigation of geologically produced antineutrinos with KamLAND*, *Nature* **436** (2005) 499.
- [210] BOREXINO collaboration, G. Bellini et al., *Observation of Geo-Neutrinos*, *Phys. Lett.* **B687** (2010) 299 [[1003.0284](#)].
- [211] J. H. Davis, *Dark Matter vs. Neutrinos: The effect of astrophysical uncertainties and timing information on the neutrino floor*, *JCAP* **1503** (2015) 012 [[1412.1475](#)].
- [212] G. B. Gelmini, V. Takhistov and S. J. Witte, *Casting a Wide Signal Net with Future Direct Dark Matter Detection Experiments*, *JCAP* **1807** (2018) 009 [[1804.01638](#)].
- [213] G. Zuzel, P. Agnes, I. Albuquerque, T. Alexander, A. Alton, D. Asner et al., *The darkside experiment: Present status and future*, in *Journal of Physics: Conference Series*, vol. 798, p. 012109, IOP Publishing, 2017.
- [214] C. E. Aalseth et al., *DarkSide-20k: A 20 tonne two-phase LAr TPC for direct dark matter detection at LNGS*, *Eur. Phys. J. Plus* **133** (2018) 131 [[1707.08145](#)].
- [215] DARKSIDE collaboration, P. Agnes et al., *Low-Mass Dark Matter Search with the DarkSide-50 Experiment*, *Phys. Rev. Lett.* **121** (2018) 081307 [[1802.06994](#)].
- [216] DARWIN collaboration, J. Aalbers et al., *DARWIN: towards the ultimate dark matter detector*, *JCAP* **1611** (2016) 017 [[1606.07001](#)].
- [217] XENON collaboration, E. Aprile et al., *First Dark Matter Search Results from the XENON1T Experiment*, *Phys. Rev. Lett.* **119** (2017) 181301 [[1705.06655](#)].
- [218] “Pico500.” <http://www.picoexperiment.com/pico500.php>.
- [219] “Pico bubble chambers.” <https://indico.fnal.gov/getFile.py/access?contribId=93&sessionId=2&resId=0&materialId=slides&confId=13702>.
- [220] SUPERCDMS collaboration, R. Agnese et al., *Projected Sensitivity of the SuperCDMS SNOLAB experiment*, *Phys. Rev.* **D95** (2017) 082002 [[1610.00006](#)].
- [221] Y. Huang, V. Chubakov, F. Mantovani, R. L. Rudnick and W. F. McDonough, *A reference earth model for the heat-producing elements and associated geoneutrino flux*, *Geochemistry, Geophysics, Geosystems* **14** (2013) 2003.
- [222] G. B. Gelmini, V. Takhistov and S. J. Witte, *Geoneutrinos in Large Direct Detection Experiments*, *Phys. Rev.* **D99** (2019) 093009 [[1812.05550](#)].
- [223] M. Honda, T. Kajita, K. Kasahara, S. Midorikawa and T. Sanuki, *Calculation of atmospheric neutrino flux using the interaction model calibrated with atmospheric muon data*, *Phys. Rev.* **D75** (2007) 043006 [[astro-ph/0611418](#)].
- [224] G. Battistoni, A. Ferrari, T. Montaruli and P. R. Sala, *The atmospheric neutrino flux below 100-MeV: The FLUKA results*, *Astropart. Phys.* **23** (2005) 526.

- [225] C. D. Carone and H. Murayama, *Possible light $U(1)$ gauge boson coupled to baryon number*, *Phys. Rev. Lett.* **74** (1995) 3122 [[hep-ph/9411256](#)].
- [226] P. Fileviez Perez, S. Ohmer and H. H. Patel, *Minimal Theory for Lepto-Baryons*, *Phys. Lett.* **B735** (2014) 283 [[1403.8029](#)].
- [227] M. Duerr and P. Fileviez Perez, *Baryonic Dark Matter*, *Phys. Lett.* **B732** (2014) 101 [[1309.3970](#)].
- [228] P. Agrawal, S. Blanchet, Z. Chacko and C. Kilic, *Flavored Dark Matter, and Its Implications for Direct Detection and Colliders*, *Phys. Rev.* **D86** (2012) 055002 [[1109.3516](#)].
- [229] D. B. Kaplan and A. Manohar, *Strange Matrix Elements in the Proton from Neutral Current Experiments*, *Nucl. Phys.* **B310** (1988) 527.
- [230] X.-d. Ji and D. Toublan, *Heavy-quark contribution to the proton's magnetic moment*, *Phys. Lett.* **B647** (2007) 361 [[hep-ph/0605055](#)].
- [231] W. Chao, *Direct detections of Majorana dark matter in vector portal*, [1904.09785](#).
- [232] P. Langacker, *Grand Unified Theories and Proton Decay*, *Phys. Rept.* **72** (1981) 185.
- [233] G. Arcadi, M. Lindner, Y. Mambrini, M. Pierre and F. S. Queiroz, *GUT Models at Current and Future Hadron Colliders and Implications to Dark Matter Searches*, *Phys. Lett.* **B771** (2017) 508 [[1704.02328](#)].
- [234] G. Arcadi, M. D. Campos, M. Lindner, A. Masiero and F. S. Queiroz, *Dark sequential Z' portal: Collider and direct detection experiments*, *Phys. Rev.* **D97** (2018) 043009 [[1708.00890](#)].
- [235] S. J. D. King, S. F. King and S. Moretti, *$SO(10)$ inspired Z' models at the LHC*, *Phys. Rev.* **D97** (2018) 115027 [[1712.01279](#)].
- [236] S. Ferrari, T. Hambye, J. Heeck and M. H. G. Tytgat, *$SO(10)$ paths to dark matter*, *Phys. Rev.* **D99** (2019) 055032 [[1811.07910](#)].
- [237] D. A. Camargo, Y. Mambrini and F. S. Queiroz, *XENON1T takes a razor to a dark E_6 -inspired model*, *Phys. Lett.* **B786** (2018) 337 [[1805.12162](#)].
- [238] P. Batra, B. A. Dobrescu and D. Spivak, *Anomaly-free sets of fermions*, *J. Math. Phys.* **47** (2006) 082301 [[hep-ph/0510181](#)].
- [239] T. Appelquist, B. A. Dobrescu and A. R. Hopper, *Nonexotic Neutral Gauge Bosons*, *Phys. Rev.* **D68** (2003) 035012 [[hep-ph/0212073](#)].
- [240] B. A. Dobrescu and C. Frugiuele, *Hidden GeV-scale interactions of quarks*, *Phys. Rev. Lett.* **113** (2014) 061801 [[1404.3947](#)].
- [241] J. A. Dror, R. Lasenby and M. Pospelov, *Dark forces coupled to nonconserved currents*, *Phys. Rev.* **D96** (2017) 075036 [[1707.01503](#)].
- [242] J. A. Dror, R. Lasenby and M. Pospelov, *Light vectors coupled to bosonic currents*, *Phys. Rev.* **D99** (2019) 055016 [[1811.00595](#)].
- [243] S. Centelles Chulia, R. Cepedello, E. Peinado and R. Srivastava, *Scotogenic Dark Symmetry as a residual subgroup of Standard Model Symmetries*, [1901.06402](#).
- [244] ATLAS, CMS collaboration, G. Aad et al., *Combined Measurement of the Higgs Boson Mass in pp Collisions at $\sqrt{s} = 7$ and 8 TeV with the ATLAS and CMS Experiments*, *Phys. Rev. Lett.* **114** (2015) 191803 [[1503.07589](#)].
- [245] K. Griest and M. Kamionkowski, *Unitarity Limits on the Mass and Radius of Dark Matter Particles*, *Phys. Rev. Lett.* **64** (1990) 615.

[246] J. Smirnov and J. F. Beacom, *TeV-Scale Thermal WIMPs: Unitarity and its Consequences*, [1904.11503](#).

[247] M. D. Schwartz, *Quantum Field Theory and the Standard Model*. Cambridge University Press, 2014.

A Partial Wave Unitarity

Following the arguments described in Ref [245] (see also Ref. [246]), it is possible to use considerations involving partial wave unitarity to derive a model-independent upper bound on the mass of the dark matter. While limited exceptions to these conclusion can be found in models in which the dark matter annihilates through a narrow resonance, for example, these constraints are quite general, and cover a wide range of dark matter candidates that are thermal relics of the early universe.

The thermal relic abundance of a species is given by the following:

$$\begin{aligned} \Omega_\chi h^2 &\simeq \frac{(n+1)x_f 1.07 \times 10^9 \text{ GeV}^{-1}}{g_*^{1/2} m_{\text{Pl}} \langle \sigma v \rangle_f} \\ &\simeq 0.12 \times (n+1) \left(\frac{x_f}{25} \right) \left(\frac{2 \times 10^{-26} \text{ cm}^3/\text{s}}{\langle \sigma v \rangle_f} \right), \end{aligned} \quad (\text{A.1})$$

where, g_* is the effective number of degrees of freedom at freeze-out, $m_{\text{Pl}} = 1.22 \times 10^{19} \text{ GeV}$ is the Planck mass, $x_f \equiv m_\chi/T_f \approx 25$, T_f is the temperature at freeze-out, and n is defined such that $\langle \sigma v \rangle_f \propto v^n$. Expanding the cross section in terms of partial waves, $\sigma = \sum_j \sigma_j$, the requirement of unitarity imposes the following constraint (for each j):

$$\sigma_j v \leq \frac{4\pi(2j+1)}{m_\chi^2 v} \approx 6 \times 10^{-23} \sqrt{x_f} \text{ cm}^3/\text{sec} \left(\frac{m_\chi}{1 \text{ TeV}} \right)^{-2}. \quad (\text{A.2})$$

We see that $j = 0$ imposes the strongest constraint. Combining Eq. (A.1) and Eq. (A.2), we arrive at the following:

$$m_\chi \leq 117 \text{ TeV} \left(\frac{\Omega_\chi h^2}{0.12} \right)^{1/2} \left(\frac{2}{g_{\text{dof}}} \right)^{1/2} \left(\frac{25}{x_f} \right)^{1/4}, \quad (\text{A.3})$$

where $g_{\text{dof}} = 2(4)$ for a thermal relic that is a Majorana (Dirac) fermion.

While the well-known constraint of Eq. (A.3) is powerful and quite general, one can also apply arguments based on partial wave unitarity to specific models, deriving in some cases even more stringent constraints. More specifically, for a particular process with a scattering matrix element, $M(\theta)$, the requirement of partial wave unitarity states that

$$\sum_{j=0}^{\infty} (2j+1) \text{Im}(a_{\mu\mu'}^j) \geq \frac{2|\vec{p}_i|}{E_{CM}} \sum_{j=0}^{\infty} (2j+1) |a_{\mu\mu'}^j|^2, \quad (\text{A.4})$$

where j is the total angular momentum quantum number, μ (μ') are defined as $\mu = \frac{1}{2}(\lambda_2 - \lambda_1)$ and $\mu' = \frac{1}{2}(\lambda_2' - \lambda_1')$, given the spin of the initial (final) state fermions λ (λ') [247]. The coefficients in the angular momentum expansion of the matrix element, $M_{\mu\mu'}(\theta)$, are given by

$$a_{\mu\mu'}^j = \frac{1}{32\pi} \int_{-1}^1 d(\cos(\theta)) d_{\mu\mu'}^j M_{\mu\mu'}(\theta), \quad (\text{A.5})$$

where $d_{\mu\mu'}^j$ are the Wigner (small) d -matrices [127]. The first two matrices are $d_{0,0}^0 = 1$, and

$$d_{\mu,\mu'}^1 = \begin{pmatrix} \cos^2\left(\frac{\theta}{2}\right) & -\sqrt{2}\cos\left(\frac{\theta}{2}\right)\sin\left(\frac{\theta}{2}\right) & \sin^2\left(\frac{\theta}{2}\right) \\ \sqrt{2}\cos\left(\frac{\theta}{2}\right)\sin\left(\frac{\theta}{2}\right) & \cos(\theta) & -\sqrt{2}\cos\left(\frac{\theta}{2}\right)\sin\left(\frac{\theta}{2}\right) \\ \sin^2\left(\frac{\theta}{2}\right) & \sqrt{2}\cos\left(\frac{\theta}{2}\right)\sin\left(\frac{\theta}{2}\right) & \cos^2\left(\frac{\theta}{2}\right) \end{pmatrix}. \quad (\text{A.6})$$

In the Majorana case and in the absence of a scalar, this can be used to set bounds on the strength of the couplings. Taking the $j = 0$ term for dark matter self-scattering in the center-of-momentum frame, $\chi\chi \rightarrow \chi\chi$, Eq. (A.4) becomes

$$|\text{Re}(a_{00}^0)| \leq \frac{1}{2v}. \quad (\text{A.7})$$

To evaluate this expression, only the $\mu = \mu' = 0$ amplitude is needed. The s , t , and u -channel diagrams contribute to the amplitude and we get the following expression:

$$M_{0,0}(\theta) = \frac{-8g_\chi^2 p^2 (1 - \cos(\theta)) \left(\frac{2m_\chi^2}{m_{Z'}^2} - 1\right)}{-p^2(1 - \cos(\theta)) - m_{Z'}^2 + im_{Z'}\Gamma} + \frac{8g_\chi^2 p^2 (1 + \cos(\theta)) \left(\frac{2m_\chi^2}{m_{Z'}^2} - 1\right)}{-p^2(1 + \cos(\theta)) - m_{Z'}^2 + im_{Z'}\Gamma} + \frac{16g_\chi^2 m_\chi^2 \left(\frac{s}{m_{Z'}^2} - 1\right)}{s - m_{Z'}^2 + im_{Z'}\Gamma}. \quad (\text{A.8})$$

Performing the integral in Eq. (A.5), the $j = 0$ coefficient is given by

$$a^0 = \frac{-g_\chi^2 m_\chi^2 (m_\chi^2 (4 + v^2) - m_{Z'}^2)}{m_{Z'}^2 \pi (m_{Z'} (m_{Z'} - i\Gamma) - m_\chi^2 (4 + v^2))}. \quad (\text{A.9})$$

Finally, the unitarity condition is given by the following:

$$g_\chi^2 \leq \frac{\pi m_{Z'}^2}{2m_\chi^2 v} \left(1 + \frac{\Gamma^2 m_{Z'}^2}{(m_{Z'}^2 - m_\chi^2 (v^2 + 4))^2} \right). \quad (\text{A.10})$$

Note that for $v \rightarrow 1$ and $\Gamma \rightarrow 0$, this bound converges to the result presented in Ref. [127], $g_\chi^2 \leq \pi m_{Z'}^2 / 2m_\chi^2$. At freeze-out, however, $v \approx \sqrt{6}/x_f$ and $x_f \approx 25$, leading this bound to be relaxed by a factor of ~ 2 . In the Dirac case, we find that this calculation yields a constraint that is less stringent than that shown in Eq. (A.3).

When a scalar is present in the theory, the constraints on the couplings relax. Repeating the above calculation for $\rho\rho \rightarrow \rho\rho$ scattering, we get the following bound on the mass of the scalar [127]:

$$m_\rho \leq \frac{\sqrt{\pi} m_{Z'}}{g_\chi}. \quad (\text{A.11})$$

Throughout this work, we set the value of m_ρ such that it saturates this bound, in order to minimize the phenomenological consequences of this particle.